HHS Public Access
Author manuscript

Acquisition of Cancer Stem Cell-like Properties in Human Small Airway Epithelial Cells after a Long-term Exposure to Carbon Nanomaterials

Chayanin Kiratipaiboon,
Department of Pharmaceutical Sciences, West Virginia University, Morgantown, West Virginia, 26506, United States

Todd A. Stueckle,
Health Effects Laboratory Division, National Institute for Occupational Safety and Health, Morgantown, West Virginia, 26505, United States

Rajib Ghosh,
Department of Pharmaceutical Sciences, West Virginia University, Morgantown, West Virginia, 26506, United States

Liying W. Rojanasakul,
Health Effects Laboratory Division, National Institute for Occupational Safety and Health, Morgantown, West Virginia, 26505, United States

Yi Charlie Chen,
College of Science, Technology and Mathematics, Alderson Broaddus University, Philippi, West Virginia, 26416, United States

Cerasela Zoica Dinu,
Department of Chemical Engineering, West Virginia University, Morgantown, West Virginia, 26506, United States

Yon Rojanasakul
Department of Pharmaceutical Sciences and WVU Cancer Institute, West Virginia University, Morgantown, West Virginia, 26506, United States

Abstract

*Address correspondence to: Yon Rojanasakul, West Virginia University, Morgantown, WV, 26506, USA. Phone: 304-293-1476. Fax: 304-293 2576, yrojan@hsc.wvu.edu.

Cancer stem cells (CSCs) are a key driver of tumor formation and metastasis, but how they are affected by nanomaterials is largely unknown. The present study investigated the effects of different carbon-based nanomaterials (CNMs) on neoplastic and CSC-like transformation of human small airway epithelial cells and determined the underlying mechanisms. Using a physiologically relevant exposure model (long-term/low-dose) with system validation using a human carcinogen, asbestos, we demonstrated that single-walled carbon nanotubes, multi-walled carbon nanotubes, ultrafine carbon black, and crocidolite asbestos induced particle-specific anchorage-independent colony formation, DNA-strand break, and p53 downregulation, indicating genotoxicity and carcinogenic potential of CNMs. The chronic CNM-exposed cells exhibited CSC-like properties as indicated by 3D spheroid formation, anoikis resistance, and CSC markers expression. Mechanistic studies revealed specific self-renewal and epithelial-mesenchymal transition (EMT)-related transcription factors that are involved in the cellular transformation process. Pathway analysis of gene signaling networks supports the role of SOX2 and SNAI1 signaling in CNM-mediated transformation. These findings support the potential carcinogenicity of high aspect ratio CNMs and identified molecular targets and signaling pathways that may contribute to the disease development.

Graphical Abstract
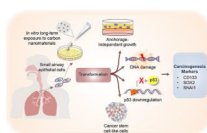
Carbon nanomaterials and asbestos fibers induce genotoxicity and cancer stem cell-like transformation in human small airway epithelial cells.

Keywords

carbon nanomaterials; cancer stem cells; carcinogenicity; small airway epithelial cells

Introduction

Carbon-based nanomaterials (CNMs), including carbon nanotubes (CNTs), are a major class of engineered nanomaterials with unique physicochemical properties such as high tensile strength, thermal conductivity, and electrical properties. Massive scale of CNMs are being produced for various applications ranging from household products, industrial processes, and biomedical applications.[1, 2] Consequently, continuous increases in occupational and environmental exposure to CNMs are expected over the coming years.[3] Importantly, respirable size (i.e. <1 μm or <4 μm aerodynamic diameter)[4] and low density of CNMs make them airborne and deposit in the lungs, potentially causing harmful effects to humans. CNTs, including single-walled carbon nanotubes (SWCNT) and multi-walled carbon nanotubes (MWCNT), have been shown to migrate into the alveolar interstitial compartment of the lungs where low clearance rate is anticipated;[5–7] hence such biopersistence could lead to chronic adverse effects such as pulmonary fibrosis.[8, 9]

The carcinogenic potential of long-term exposure to CNTs has been reported,[10, 11] possibly due to their high aspect ratio and biopersistence features shared with asbestos (ASB), which is a known human carcinogen causing lung cancer and mesothelioma.[12] Furthermore, *in vitro* studies have reported DNA damage-inducing activity of CNTs.[13, 14] These studies demonstrated that SWCNT and MWCNT can incorporate into mitotic spindle apparatus of human airway epithelial cells which resulted in aneuploid chromosomes.[13, 14] Similarly, intratracheal instillation of flake-like shaped carbon nanoparticles, ultrafine carbon black (UFCB), was shown to cause DNA strand break in C57BL/6 mice.[15] Since chromosome aberration and DNA damage underlie carcinogenic development,[16] these studies suggest the carcinogenic potential of CNTs and UFCB. Experimental animal studies showed that pharyngeal aspiration of SWCNT increased the incidence of mutant K-*ras*, which is a known oncogenic driver of lung carcinogenesis.[17, 18] Moreover, an increased incidence of mesothelioma has been reported in p53 heterozygous knockout mice after receiving an intraperitoneal injection of MWCNT.[19] MWCNT was also shown to increase cell migration and upregulate the expression of carcinogenesis-related genes including vascular endothelial growth factor A (VEGFA), sonic hedgehog signaling (SHH) molecule, smoothened (SMO), mitogen-activated protein 3-kinase 20 (MAP3K20), nitric oxide synthase 2 (NOS2), GLI family zinc finger 1 (GL1) and prostaglandin-endoperoxide synthase 2 (PTGS2) in human small airway epithelial cells (SAECs).[20] Co-culture of SAECs and human vascular endothelial cells (HMVECs) has been reported to promote angiogenesis of HMVECs after SAEC exposure to MWCNT,[21] suggesting the pro-carcinogenic effect of MWCNT. With regards to other nanomaterials, an intratracheal instillation or pulmonary inhalation of titanium dioxide nanoparticles was shown to increase lung cancer incidence in rodents,[22–24] although epidemiological studies found no clear relationship between the occupational exposure and risk of lung cancer.[25–27] Moreover, zinc oxide nanoparticles were shown to upregulate tumor suppressor protein p53, cyclin dependent kinase inhibitor 1A (CDKN1A), c-Jun N-terminal kinases (JNKs) in lymphocytes isolated from lung cancer patients,[28] however their carcinogenicity has not been established. Recently, our group has demonstrated the ability of SWCNT and MWCNT to induce neoplastic transformation in human lung epithelial cells after a long-term exposure in culture.[29, 30] These animal and *in vitro* studies support the potential carcinogenicity of CNMs, however the underlying mechanisms and *in vitro* models for carcinogenicity testing of CNMs are not well understood or lacking.

Emerging evidence indicates that cancer stem cells or stem-like cells (CSCs), a subpopulation of cancer cells residing within a tumor, are the main driving force of tumor formation and metastasis due to their self-renewal and unlimited replicative capabilities.[31] Several lines of evidence suggest that CSC phenotypes are maintained through the sustained level of self-renewal and epithelial-mesenchymal transition (EMT) related transcription factors.[32–35] Overexpression of self-renewal transcription factors such as Octamer-binding transcription factor 4 (Oct-4), Nanog homeobox (NANOG), and Sex determining region Y-box 2 (SOX2) has been reported in CSCs of many cancer types.[36–39] OCT4 and NANOG expression, in particular, has been associated with worse clinical outcomes and poor survival outcome in lung cancer patients.[40, 41] A recent study indicates that SOX2 is overexpressed in various types of lung cancer[42, 43] and that silencing this transcription factor resulted in

decreased oncogene expression in a xenograft model using non-obese diabetic/severe combined immunodeficiency (NOD/SCID) mice.[44] Similarly, overexpression of EMT-activating transcription factors including zinc finger E-box binding homeobox 1 (ZEB1), snail family transcriptional repressor 1 (SNAI1) and snail family transcriptional repressor 2 (SNAI2) have been reported to promote the occurrence and progression of lung cancer.[35, 45, 46] For instance, ZEB1 was shown to be an important biomarker for early detection of oncogenesis in lung epithelial cells, and overexpression of this transcription factor promoted metastasis of transformed human bronchial epithelial cells.[45] Silencing SNAI1 expression in non-small cell lung cancer cells led to growth inhibition via upregulation of tumor suppressor p21.[46] Overexpression of SNAI2 was also observed in lung CSCs which was shown to promote tumor metastasis in human lung carcinoma.[35] Despite the growing evidence for the role of CSC-related transcription factors in lung carcinogenesis, the participation of these transcription factors in nanomaterial-induced carcinogenesis has not been investigated.

To date, there are very limited studies on the long-term adverse effects of CNMs.[29, 30] The present study aims to investigate such effects with a focus on DNA double-strand break, neoplastic and CSC-like transformation in human small airway epithelial cells (SAECs). We continuously exposed the cells to low-dose SWCNT, MWCNT, UFCB, and ASB over a long period to mimic the gradual cellular transformation process during carcinogenesis. We demonstrated that such exposure induced particle type-dependent DNA double-strand break, possibly via p53 downregulation, and neoplastic and CSC-like transformation. We also investigated the underlying mechanisms of transformation and identified key self-renewal and EMT transcription factors and signaling that may be involved in the process.

Materials and methods

Materials and characterization

Characterization of materials including elemental content analysis, surface area, zeta potential and particle size measurements were conducted and the results are summarized in Table 1. SWCNT (CNI, Houston, TX), MWCNT (MWNT-7, lot #05072001K28; Mitsui & Company, Tokyo, Japan), UFCB (Elftex 12; Cabot, Edison, NJ), and ASB (Crocidolite, CAS 12001-28-4; National Institute of Environmental Health Sciences, Research Triangle Park, NC) were analyzed for elemental contents by nitric acid dissolution and inductive coupled plasma-atomic emission spectroscopy. Surface area of SWCNT, MWCNT, UFCB, and ASB was analyzed by Brunauer Emmett Teller (BET) nitrogen adsorption technique. Particle dimensions were assessed by electron microscopy. Dynamic light scattering (DLS) measurements of average hydrodynamic diameter were performed with a NanoSight NS300 (Malvern Instrument, Worcestershire, UK). All particles were dispersed in cell culture medium and DLS measurements were conducted using scattering angle of 90° with an argon ion laser set at excitation wavelength of 488 nm. Zeta potential was measured using a Zetasizer Nano ZS90 (Malvern Instrument). Particle were dispersed in cell culture medium and equilibrated inside the instrument for 2 min, and five measurements (10 sec delay between measurements) each consisting of five runs (2 sec delay between runs) were recorded.

Material preparation

All test materials were kept as a dry powder in tightly closed containers at 4 °C and freshly dispersed in phosphate-buffered saline (PBS) to obtain stock solutions at 0.1 mg/mL. A natural lung surfactant, Survanta® (Abbott Laboratories, Columbus, OH, USA), was then added to SWCNT, MWCNT, and UFCB stock solutions at the concentration of 150 μg/mL to aid particle dispersion. All particle preparations were sonicated using light sonication (Sonic Vibra Cell Sonicator, Sonic & Material Inc., Newtown, CT, USA) with the power, frequency and amplitude settings of 130 W, 20 kHz and 60% for 10 seconds, followed by a dilution with cell culture medium to the exposure dose. The concentration of Survanta® used in this study was shown to cause no cellular toxicity or neoplastic transformation.[47]

Cell culture and sub-chronic exposure

Primary human small airway epithelial cells immortalized with hTERT (SAECs) were kindly provided by Dr. Tom Hei (Columbia University, New York, NY, USA).[48] SAECs were grown in small airway epithelial cell growth basal media (SABM) supplemented with Clonetics SAGM SingleQuots (Lonza, Walkersville, MD, USA) containing 0.4% bovine pituitary extract, 0.1% insulin, 0.1% hydrocortisone, 0.1% retinoic acid, 1% bovine serum albumin, 0.1% transferrin, 0.1% triiodothyronine, 0.1% epinephrine, 0.1% human epidermal growth factor and 0.1% gentamicin. Cells were continuously exposed to 0.02 μg/cm^2 of SWCNT, MWCNT, UFCB or ASB for 6 months and maintained at 37 °C in a humidified 5% CO_2 as previously reported.[20] The cells were passaged weekly at pre-confluent densities using a solution containing 0.05% trypsin and 0.5 mM EDTA (Invitrogen, Carlsbad, CA). Passage-matched cells were exposed to the dispersant for 6 months utilized as control cells.

Soft agar colony formation assay

The bottom layer of agar medium (0.5%) was prepared by mixing 1:1 mixture of 1% agarose and 2× concentrate MEM medium (Lonza) containing 15% fetal bovine serum (FBS) and 1% gentamicin at 44 °C. Each growth factor from the SAGM SingleQuots kit (Lonza) was added to the warm agar to obtain the corresponding concentration of their normal growth medium. The bottom layer of agar medium (600 μL) was added and allowed to solidify for 30 minutes in a 24-well plate. The upper layer was prepared by suspending 3×10^3 cells in 0.33% agar medium (200 μL). Next, normal growth medium of SAECs (300 μL) was added over the upper layer after it was solidified at 37 °C and replaced with fresh culture medium every three days. Colony formation was captured under a microscope (Keyence BZ-X700; Osaka, Japan). Relative colony number and surface area were calculated by dividing the values of particle-exposed cells by that of passage-matched control cells.

Immunofluorescence

Cells were seeded on a cover slip at the density of 1.5×10^4 cells per well in 24-well plates with a total volume of 500 μL. After a 48-h incubation period, cells were fixed with 4% paraformaldehyde and permeabilized with 0.25% Triton-X for 10 min at room temperature. After that, the cells were blocked with a medium containing 0.5% saponin, 1% FBS, and 1.5% goat serum, and incubated with primary antibodies against CD133 (1:200 dilution, Thermo Fisher Scientific, Waltham, MA), phosphorylated histone H2AX (γ-H2AX; 1:300

dilution, Millipore Sigma, Burlington, MA), and β-actin (1:3,000 dilution, Cell Signaling Technology, Danvers, MA) overnight at 4 °C. The cells were then incubated with AlexaFluor 488 and 647-conjugated secondary antibodies (1:500 dilution, Thermo Fisher Scientific, Waltham, MA) for 1 h at room temperature, and mounted in DAPI-containing medium (Vector Laboratories Inc, Burlingame, CA). Immunofluorescence images were acquired using Keyence BZ-X700 fluorescence microscope and quantified using an image J analysis software.

Immunoblotting

Cells were seeded at the density of 1.5×10^5 cells per well in 6-well plates with a total volume of 2 mL. After a 48-hour incubation period, the cells were lysed with ice-cold lysis buffer containing 20 mM Tris–HCl (pH 7.5), 1% Triton X-100, 150 mM NaCl, 10% glycerol, 1 mM Na_3VO_4, 50 mM NaF, 100 mM phenylmethylsulfonyl fluoride, and a commercial protease inhibitor mixture (Roche Molecular Biochemicals, Indianapolis, IN) for 40 minutes. Cell lysates were determined for protein content using the Bradford assay kit (Bio-Rad Laboratories, Hercules, CA). Equal amounts of denatured proteins (40 μg) were loaded onto 7.5–10% sodium dodecyl sulfate-polyacrylamide gel electrophoresis (SDS-PAGE) and transferred onto nitrocellulose membranes (Bio-Rad). The transferred membranes were blocked in 5% nonfat dry milk in TBST (25 mM Tris–HCl, pH 7.4, 125 mM NaCl, 0.05% Tween 20) for 1 hour and incubated with primary antibodies against CD133, p53, CD44, ABCG2, OCT4, NANOG, SOX2, ZEB1, SNAI1, SNAI2 and GAPDH (Cell Signaling Technology, Danvers, MA) at 4°C overnight. Membranes were washed twice with TBST for 10 minutes and incubated with HRP-coupled isotype-specific secondary antibodies (Cell Signaling Technology, Danvers, MA) for 1 hour at room temperature. The immune complexes were detected by an enhanced chemiluminescence detection system (Millipore Corporation, Billerica, MA) and quantified using image J densitometry software.

Anoikis and apoptosis assays

Cells were detached and made into single-cell suspension in growth factor-free SABM medium. The suspended cells were then plated onto a 6-well ultralow attachment plate at the density of 1×10^5 cell/mL with a total volume of 2 mL and incubated for 60 h. The cells were harvested at various times (0–60 h) to assess cell viability using MTS assay (Promega, Madison, WI), according to the manufacturer's protocol. Apoptosis of the suspended cells was determined by Hoechst 33342 assay (Molecular Probes, Eugene, OR). After 12 h, the above single-cell suspension in 6-well ultralow attachment plate were seeded on to 96-well ultralow attachment plate with a total volume of 200 μL. Cells were incubated with 10 μg/mL Hoechst 33342 for 30 min at 37 °C and visualized under a fluorescence microscope. Cells with intense nuclear fluorescence were considered apoptotic. . The percentage of apoptosis was calculated from 10 random fields from approximately 1,000 nuclei for each sample.

Spheroid formation assay

Spheroid formation was performed under stem cell-selective culture conditions as previously described.[49] Cells were detached and resuspended in 0.8% methylcellulose (MC)-based serum-free medium (Stem Cell Technologies, Vancouver, Canada) containing 20 ng/mL

epidermal growth factor (EGF; BD Biosciences, San Jose, CA), basic fibroblast growth factor (bFGF), and 4 μg/mL insulin (Sigma). Cells at the density of 1×10^4 cell/well were plated onto an ultralow attachment 24-well plate with a total volume of 600 μL and cultured for 4 weeks. EGF and bFGF (20 ng/mL) and insulin (4 μg/mL) were added every three days. The culture medium was replaced with fresh 0.8% MC-based serum-free medium supplemented with growth factors as described above once a week. Spheres were harvested, dissociated into single cell suspensions, and cultured under stem cell-selective conditions to form secondary spheroids. Relative spheroid numbers and areas were calculated by dividing the values of particle-exposed cells by passage control cells

Pathway Analysis

Whole genome mRNA microarray datasets from our previous work[20] were uploaded into Ingenuity Pathway Analysis (Qiagen) to investigate the roles of SOX2-associated CSC- and EMT-associated signaling in CNM-exposed cells. Roles for SOX2 in ranked cellular functions, upstream regulator, and signaling networks were searched within the results of the Core Analysis. For those functions and networks with SOX2, all genes associated with the function were plotted to investigate signaling relationships and potential relationships with previously identified pro-cancer signaling in each cell type.[20] For those transformed cells that did not show over-expressed SOX2, we investigated other transcriptional regulators including SNAI1. Meaningful signaling networks were overlaid with mRNA differential expression and Z-score-based activation/inhibition prediction values (Z $\geq$ ±2).

Statistical analysis

Data are presented as the means S.D. from at least three independent experiments. Statistical differences were determined using two-way ANOVA and post hoc Tukey's test for multiple comparison at a significance level (α) of 0.05.

Results and discussion

Material characterization

Physiochemical properties of all test nanoparticles are summarized in Table 1. Electron microscopic characterization of all test particles was performed and reported previously by our group.[30] SWCNT (CNT, Houston, TX) were produced by high-pressure carbon monoxide (HiPco) technique. They were purified to remove metal contaminants using acid treatment. Elemental analysis by nitric acid dissolution and inductive coupled plasma-atomic emission spectroscopy showed that the SWCNT contained 99% elemental carbon and 0.23% iron. Surface area was assessed by Brunauer Emmet Teller (BET) method and was 400–1,040 m^2/g. The length and width of individual SWCNT as determined by field emission scanning electron microscopy were 1–4 μm and 1–4 nm, respectively. Particle agglomerate or hydrodynamic diameter measured by DLS and zeta potential of SWCNT in culture medium were 122.5 nm and −17.1 mV, respectively. The nanomaterial was previously characterized by Wang *et al.*[47] and Sargent *et al.*[13] MWCNT (MWNT-7, lot #05072001K28; Mitsui & Company, Tokyo, Japan) was synthesized by chemical vapor deposition. Elemental analysis of MWCNT indicated 99% elemental carbon and 0.32% iron. BET surface area was 26 m^2/g. Length and width obtained from field emission scanning electron microscopy of

individual MWCNT was 8.19 ± 1.7 µm and 81 ± 5 nm, respectively. Hydrodynamic diameter and zeta potential of MWCNT in culture medium were 163.3 nm and −17.6 mV, respectively. Hydrodynamic size of non-spherical particles such as CNTs and asbestos fibers should be taken with caution and only as an estimate of their hydrodynamic size. Detailed characterization of MWCNT was described by Pacurari *et al.*[50], Porter *et al.*[51], and Mishra *et al.*[52] UFCB (Elftex 12; Cabot, Edison, NJ) was synthesized by vapor-phase pyrolysis. Content of UFCB was 99% elemental carbon and 0.0011% iron. BET surface area and width of individual UFCB were 43 m^2/g and 37 nm, respectively. Length was not applicable (i.e. spherical shaped based on electron microscopic observations). Hydrodynamic diameter and zeta potential of UFCB in culture medium were 126.7 nm and −15.4 mV, respectively. UFCB was previously characterized by Wang *et al.*[47] ASB (Crocidolite, CAS 12001-28-4) was from the National Institute of Environmental Health Sciences (Research Triangle Park, NC) and was characterized by Msiska *et al.*[53] Elemental analysis of ASB was 50.9% SiO_2, 31.8% iron and less than 1% carbon. BET surface area, length and width of individual ASB were 9.8 m^2/g, 10 µm and 210 nm, respectively. Hydrodynamic diameter and zeta potential of ASB in culture medium were 144.9 nm and −18.4 mV, respectively.

Chronic CNM exposure induces irreversible neoplastic-like transformation and DNA double-strand break

Our group previously demonstrated that Survanta®-dispersed SWCNT (SD-SWCNT) have a smaller sized structure compared to PBS-dispersed particle (ND-SWCNT). SD-SWCNT elicited a cell growth-stimulating effect but induced a suppressive effect at high doses. On the other hand, ND-SWCNT showed no effect, suggesting that dispersion status of particles is essential to their bioactivities. We also found that the concentration of Survanta® used in this study does not mask the bioactivity of SWCNT or cause cytotoxicity.[47] Therefore, Survanta® dispersion method was employed to improve the dispersion of all tested CNMs. The dispersion of CNMs in culture medium was observed under a microscope and an average agglomerate size and zeta potential of the particles were determined using DLS as shown in Table 1. Human small airway epithelial cells (SAECs) were continuously exposed to non-cytotoxic concentration of SWCNT, MWCNT, UFCB or ASB at 0.02 µg/cm^2 and passaged weekly for a period of 6 months as previously described.[30] The nanomaterial dose used in this study was calculated based on the lowest *in vivo* dose of CNTs that caused biological response in mice (10 µg/mouse)[5, 7] normalized to the average mouse alveolar surface area (~500 cm^2)[54], indicating an *in vitro* surface area dose of 0.02 µg/cm^2. ASB was used in this study as a carcinogenic particle control with similar morphology to CNTs. To assess the carcinogenic potential of CNMs, the exposed cells were examined for their ability to form colonies under non-adherent conditions, which is a phenotypic characteristic of cancer cells.[55] The cells were grown on soft agar and colony formation was determined at 28 days post-plating. Consistent with the previous reports by our group in human bronchial (BEAS-2B) and small airway epithelial cells.[29, 30] SWCNT-exposed BEAS-2B cells, SWCNT- and MWCNT-exposed SAECs were able to form significantly more and larger colonies as compared to control cells which formed very few small colonies at 6 months post-exposure. ASB- and SWCNT-exposed cells formed the highest number of colonies, followed by MWCNT- and UFCB-exposed cells, respectively (Fig. 1A–C). Less colony formation of the control cells was first observed at 14 days post-plating. This is likely due to

an inability of normal cells to grow and form spheroids under non-adherent conditions, whereas transformed cells possess this ability due to the activation of oncogenic signaling pathways.[56] Since the exposed cells were maintained in normal cell culture medium without the particles for at least ten passages before testing, these results indicate that long-term exposure to CNMs induced irreversible neoplastic-like transformation in human small airway epithelial cells similar to that observed with ASB.

Sustained DNA damage is frequently associated with carcinogenic transformation[16] and failure to repair DNA lesions, particularly double-strand breaks (DSBs), may contribute to genomic instability and cancer development.[16] In case of particle-induced carcinogenesis, it was shown that ASB was able to induce DNA strand breaks in pleural mesothelial cells,[57] which is believed to contribute to its pathogenicity. In this study, we investigated the ability of CNMs to induce DNA strand breaks in the exposed lung cells by measuring phosphorylated histone H2AX (γ-H2AX) foci, a widely accepted biomarker for DSB.[58] Fig. 1D,E shows that like ASB-exposed cells, SWCNT-, MWCNT- and UFCB-exposed cells exhibited a significant increase in γ-H2AX-positive cells (>5 foci/cell)[59] as compared to control cells. The magnitude of induction was quite comparable among the tested particles, with SWCNT-exposed cells exhibiting the most significant change. SWCNT and MWCNT were previously shown to induce mitotic spindle alterations and chromosomal aneuploidy in primary and immortalized human airway epithelial cells.[13, 14] Likewise, pulmonary administration of UFCB (Printex 90) in C57BL/6 mice caused substantial DNA damage in bronchoalveolar lavage and lung tissue cells.[15] These findings support the genotoxicity and carcinogenic potential of the tested CNMs. Indeed, MWCNT (Mitsui-7) and UFCB are currently classified as a group 2B carcinogen by the International Agency for Research on Cancer, whereas other CNTs were non-classifiable due to the lack of sufficient evidence for their carcinogenicity.

p53 is a tumor suppressor protein that is involved in DNA repair process and functions to protect the genome from mutations and genomic aberrations.[60] Loss of function and/or mutation of p53 has been regarded as a predisposing factor for tumor initiation.[61] In this study, we investigated the effect of long-term CNM exposure on p53 expression in human SAECs by immunoblotting. Fig. 1F,G shows that p53 expression was substantially downregulated in SWCNT-, MWCNT-, UFCB- and ASB-exposed cells as compared to control cells, with the effect being most pronounced in SWCNT-exposed cells. These results are in good agreement with our previous finding showing a significant decrease in basal p53 expression in CNT- and ASB-exposed cells.[30] However, the expression of phospho-p53 in these cells remained intact, suggesting the preservation of p53 functionality in these cells. In bronchial epithelial BEAS-2B cells, however, the level of phospho-p53 was decreased upon long-term exposure to SWCNT.[29] Since BEAS-2B cells have dysregulated p53 expression as a result of SV40-mediated immortalization, these results suggest that cell immortalization could result in attenuated phospho-p53 in the exposed cells. Together, our results demonstrated the DNA-damaging effect of chronic CNM exposure in SAECs and provided a possible mechanism of particle-induced DNA damage through p53 downregulation.

Chronic exposure to CNMs induces CSC-like phenotype

Cancer stem cells (CSCs) are defined by their fundamental properties of self-renewal, tumor-initiating capacity, and ability to give rise to more differentiated progeny.[62] It was evidenced that CSCs are able to survive and proliferate to form spheroid structures under non-adherence in serum-free media known as stem-cell selective conditions.[49] In this study, we examined the effect of CNMs on CSC-like phenotypes in SAECs by anoikis (detachment-induced apoptosis) and spheroid formation assays. In anoikis assay, cells were detached, suspended in serum-free medium, and incubated for 60 hours in non-adherent poly-HEMA-coated plates. The cells were then collected and evaluated for cell survival at different time points by MTS assay. Fig. 2A shows that as compared to passage-matched control cells whose survival gradually decreased over time, SWCNT-, MWCNT- and UFCB-exposed cells exhibited death (anoikis) resistance, as indicated by their increased survival under non-adherent conditions. Similar to ASB-exposed cells, SWCNT- and MWCNT-exposed cells were able to retain anoikis resistance at 9–60 hours after cell detachment, whereas UFCB-exposed cells exhibited anoikis resistance at 9–12 hours (Fig. 2A). We also evaluated apoptosis of the exposed cells by Hoechst 33342 assay, which detects DNA condensation and fragmentation, a morphologic characteristic of apoptotic cells. Fig. 2B,C shows that all CNM- and ASB-exposed cells exhibited apoptosis resistance relative to control cells, as indicated by their fewer number of Hoechst 33342-positive cells at 12 hours post-detachment. ASB- and SWCNT-exposed cells were found to be most resistant, followed by MWCNT- and UFCB-exposed cells, respectively (Fig. 2A–C). These results are consistent with our previous studies showing apoptosis resistance of SWCNT-transformed cells to various agents including etoposide, antimycin A, Fas ligand, and tumor necrosis factor-α (TNF-α).[29, 63]

To substantiate the effect of CNMs on stem properties of SAECs, we tested the ability of CNM- and ABS-exposed cells to induce 3D spheroid formation in culture. The nanomaterial-exposed cells were detached and seeded at a low density onto non-adherent plates. The primary spheroids were allowed to form in serum-free media for 21 and 28 days. Fig. 2D–F shows that SWCNT-, MWCNT-, UFCB- and ASB-exposed cells were able to form significantly more spheroids than control cells. We also determined the effect of long-term particle exposure on secondary spheroid formation. In this study, primary spheroids were detached, resuspended in serum free media, and grown under non-adherent conditions for another 21 and 28 days. Fig. 2G–I depicts the number of secondary spheroids formed at the two time points, showing a significantly higher number of spheroids formed by ASB- and SWCNT-exposed cells, followed by MWCNT- and UFCB-exposed cells, as compared to control cells. This is in accordance with our previous findings that formation of primary and secondary spheroids was strikingly increased in chronic SWCNT-exposed BEAS-B cells at 14 days after plating.[64] These results support our earlier finding and indicate the ability of ABS- and CNM-exposed cells to self-renew and exhibit CSC-like properties.

Chronic CNM exposure upregulates CSC markers

CD133 is a commonly used biomarker for lung CSCs,[65] and its high expression in lung cancer patients has been associated with poor survival outcome[65] and short disease free period.[66] CD133-positive lung cancer cells were reported to possess self-renewal and

unlimited proliferative capabilities, whereas these characteristics were absent in CD133-negative cells.[67] In this study, we evaluated the expression of CD133 in CNM- and ASB-exposed cells to assess their stem properties by immunofluorescence staining. Fig. 3A,B shows that the expression of CD133 was significantly elevated in the secondary spheroid of CNM- and ASB-exposed cells, as compared to control cells, with the expression in SWCNT-exposed cells being the highest, followed closely by ASB- and MWCNT-exposed cells. UFCB-exposed cells expressed the lowest level, although their CD133 expression was still higher than that of the control cells. In an effort to determine the localization and distribution of stem cells in the spheroids, we performed z-stacking image analysis of fluorescently stained spheroids. Orthogonal views and 3D images were created and analyzed for CD133 expression along the z-axis. Fig. 4A,B shows that the majority of CD133-expressing cells resided in the central area of the spheroids. Such localization could be a result of less oxygen being able to diffuse through the central area of the spheroids, creating an advantageous condition for preserving CSC-like characteristic.[68]

To validate the CSC-inducing effect of CNMs, the CNM-exposed cells were analyzed for CD133 and other known CSC markers, including CD44[69] and ABCG2,[70] by Western blotting. CD44 and ABCG2 have been linked to the occurrence of lung cancer,[71, 72] but their involvement in nanoparticle-induced pathogenesis is not known. Consistent with the immunofluorescence results, our Western blot results showed an increased expression of CD133 in CNM- and ASB-exposed cells relative to control cells (Fig. 3C,D). The expression levels of CD44 and ABCG2 in these cells, however, showed no clear discernible pattern with the expression of CD44 being relatively unchanged in all CNM-exposed cells, whereas ABCG2 expression was upregulated in all but MWCNT-exposed cells. These results indicate particle type-specific regulation of stem cell markers, with CD133 as the most predictive marker of CNM-induced CSCs.

Chronic CNM exposure induces self-renewal and EMT-related transcription factors

To understand the molecular mechanisms of CNM-induced CSCs, we investigated self-renewal and EMT transcription factors, which are known to be essential to maintaining CSC functions,[33, 73] in CNM-exposed cells. Immunoblot analysis showed a substantial increase in stem cell transcription factor SOX2 in SWCNT-, MWCNT- and ASB-exposed cells, with a negative effect in UFCB-exposed cells (Fig. 5A,B). The magnitude of upregulation in SWCNT-, MWCNT- and ASB-exposed cells were 15, 2.5 and 16-fold over a control level, respectively. The expression of other self-renewal transcription factors, including OCT4 and NANOG, were relatively unchanged in all exposed cells (Fig. 5A,B), suggesting their limited role in controlling the stem properties of these cells.

In the lung, SOX2 expressing cells were shown to be responsible for tissue homeostasis and cell proliferation during injury repair.[74, 75] SOX2 expression was also reported to be elevated in lung cancer cells,[42] which promoted survival, oncogenic phenotype, and tumorigenesis of lung CSCs possibly through the upregulation of multiple oncogenes including c-Myc, Wnt1, Wnt2, and Notch1.[44] Similarly, SOX2 overexpression was found to enhance oncogenic phenotypes of lung cancer cells via a positive feedback loop of epidermal growth factor receptor and BCL2L1.[76] A recent study suggested that SOX2 overexpression led to

bronchial epithelial cell dysplasia through an upregulation of oncogenic proteins such as cyclin D1 and BCL2, which control cell cycle progression, apoptotic cell death, and tumor suppressor protein p21.[77] Therefore, strong evidence supports self-renewal and oncogenic properties of SOX2 in human lung cells, which may drive the pathogenic development of CNM- and ASB-exposed cells.

Increasing evidence also supports the role of EMT in CSC regulation and tumor progression in various cancers.[34, 78–80] EMT is a cellular transformation process that allows epithelial cells to adopt mesenchymal phenotype to increase their motility and invasiveness, which is crucial to cancer development and progression.[81] Key EMT transcription factors such as ZEB1, SNAI2, and SNAI1 have been associated with poor prognosis of lung cancer.[82–84] In this study, we evaluated the expression of ZEB1, SNAI1, and SNAI2 in CNM- and ASB-exposed cells by immunoblotting. Fig. 5C,D shows that ZEB1 was weakly upregulated in SWCNT-, MWCNT- and ASB-exposed cells, and minimally expressed in UFCB-exposed cells, as compared to control cells. SNAI2 expression was also weakly upregulated in SWCNT- and MWCNT-exposed cells, but downregulated in ASB-exposed cells (Fig. 5C,D). On the other hand, SNAI1 was highly upregulated in SWCNT-, MWCNT- and UFCB-exposed cells, but downregulated in ASB-exposed cells. These results indicate the variability and complexity of EMT-mediated regulation of CSCs by nanoparticle-induced transcription factors. Most EMT transcription factors appeared to be upregulated in SWCNT- and MWCNT-exposed cells, which may attribute to their neoplastic and CSC-like properties. ZEB1 has been shown to positively regulate anchorage-independent cell growth in lung cancer cells.[85] It also suppresses tumor suppressor genes such as Semaphorin 3F.[86] SNAI2 was reported to promote tumor angiogenesis, metastasis, and immune suppression in lung cancer cells via downregulation of 15-hydroxyprostaglandin dehydrogenase, an enzyme responsible for prostaglandin E2 degradation.[87] SNAI1 was shown to be involved in cell malignancies and its genetic knockdown repressed the proliferation rate and tumorigenicity of lung cancer cells.[46] Together, these studies support for the role of EMT-related transcription factors in neoplastic and CSC-like transformation of SAECs after a chronic exposure to CNMs and ASB.

Differential SOX2 and SNAI1 signaling associated with each high aspect ratio particle

To further investigate the potential roles of CSC- and EMT-associated genes in CNM-exposed cells, pathway analysis was conducted using whole genome mRNA expression from each exposed cell type. Based on the whole genome expression profile, Upstream Analysis in Ingenuity Pathway Analysis (IPA) predicted an activation of SOX2-OCT4-NANOG complex (Z = 2.0) in SWCNT-exposed cells (Fig. 6A). SOX2 was overexpressed by 14.3-fold while POU5F1 (OCT4) was under-expressed 6.4-fold compared to control cells. To investigate the gene signaling responsible for this prediction, all associated genes both up and downstream of this complex were plotted. Downstream over-expressed SMARCAD1 (10.1-fold) and RIF1 (5.8-fold) and downregulated PAX6 (−6.9-fold) and HOXB1 (−6.3-fold) were identified (Fig. 6A). The proteins associated with CSC signaling were added to this network (PROM1 [CD133], ABCG2, SNAI1, and SNAI2) to understand the signaling relationships with SOX2 signaling network. Activated SOX2 caused a direct overexpression of downstream SMARCAD1, PROM1, SNAI1, and NANOG with indirect activation of

RIF1. Both SMARCAD1 and RIF1 are involved in Ataxia telangiectasia mutated (ATM)-mediated DNA double strand break (DSB) repair and DNA replication repair at the 5' end. [88, 89] SMARCAD1 can contribute to naïve pluripotency in early embryo development,[90] hence suggesting that SOX2-SMARCAD1 signaling may play an important role in CSC-like phenotype in CNT-exposed cells. RIF1 is involved in stem cell pluripotency and its overexpression is associated with poor prognosis in non-small cell lung cancer (NSCLC) due to suppressed homologous recombination following DSB repair, genetic instability, and mutagenesis.[91] These findings suggest that SOX2 overexpression and activation are in response to DSB repair following chronic CNT exposure and may contribute to their neoplastic CSC-like phenotype.

Based on the overexpression of SOX2 in ASB-exposed cells, the signaling relationships associated with SOX2 involving oncogenesis and stem cell development were investigated in IPA. Cancer was identified as the top ranked cellular function in ASB-exposed cells with 236 differentially expressed genes and a Log p-value = 9.5E-6. In this signaling network, an overexpressed SOX2 was found to activate CD44 and ETV5. To further understand SOX2-associated signaling, the IPA knowledge base was queried for all known genes associated with SOX2. This network displayed unique crosstalk between cell differentiation and pro-cancer signaling (Fig. 6B). Overexpressed CD44 with overexpressed SOX2 was found in lung cancer cells following $PM_{2.5}$ exposure,[92] and promoted lung cancer in animal models by enhancing angiogenesis, migration, and apoptotic signaling.[93, 94] In addition, overexpressed ATF3, a transcriptional regulator that maintains genetic integrity under stressful conditions, indicates ASB potential damage to SAEC DNA. ATF3 overexpression was observed in NSCLC patient tumor samples.[95] Upregulated ETV5 downstream of SOX2 was found to have critical function for retaining alveolar Type II cell phenotype and associated with lung tumor initiation.[96]

Downregulated FGFR2, FN1, and LOX appeared to assist in downregulating SNAI1, suggesting that extracellular matrix influenced SOX2 activity. Decreased FGFR2 expression is associated with maintaining undifferentiated cells during lung branching development by repressing SOX2, and plays a role in cancer development.[97] LOX crosslinks collagen/elastin and may stabilize microtubules in the mitotic spindle during mitosis, thus acting as a tumor suppressor[98] while FN1 is associated with cell migration and adhesion. Overexpressed GATA3, a T-cell developmental and endothelial cell regulator, was associated with FN1 and decreased LOX and NF2. NF2 possesses tumor suppression activity, regulates cytoskeleton dynamic, and is downregulated in malignant mesothelioma, suggesting a strong link with asbestos-induced cancer.[99] Interestingly, the loss of NF2 expression may have promoted overexpressed SRC, a proto-oncogene and cancer cell invasion signaling in many cancers. [100]

Gene expression analysis showed no differential expression in SOX2 in MWCNT-exposed cells, while protein expression was mildly overexpressed (Fig. 5A,B). Based on the weak SOX2 expression and strong overexpression of SNAI1 (Fig. 5A–D), we investigated the role of SNAI1 in stem cell-associated signaling pathways and their potential role in cancer signaling. Both 'cancer of cells' and 'morphology of embryonic tissue' functions possessed overexpressed SNAI1 as a gene signaling hub in both functions' signaling networks (Fig.

6C). Only those genes associated with SNAI1 were kept in the cancer signaling network. Overexpressed MYC, FOXO1, and SNAI1 served as key hub genes in the morphology of embryonic tissue network, while SNAI1 and downregulated CXCL8 and CCL2 served as key hub genes in the cancer of cells network. To investigate the potential crosstalk between these two networks, both networks were plotted with all known associations in IPA database. Along with the overexpressed SNAI1, downregulated FOXA2, FGFR2, COL2A1, and overexpressed RNF2 were shared between the two networks.

Overexpressed genes in the embryonic tissue network were primarily involved with tumor promotion and suppression, cholesterol receptors, and differentiation, while downregulated genes were primarily associated with fibroblast and platelet-derived growth factor signaling, cytoskeleton dynamics, and differentiation. Of note, overexpressed transcriptional regulators NR4A3, FOXO1, and TCF7L1 indicate several different differentiation pathways with known roles in cancers[101, 102] that may contribute to the SNAI1-associated neoplastic phenotype in MWCNT-exposed cells. Previously, we identified MYC, FOXO1, and SNAI1 as possessing a proto-oncogene signaling function in MWCNT-exposed human SAECs,[30] which is supported by their known roles in lung adenocarcinoma and CSC regulation.[103–105] Current results suggest that embryonic development signaling of the overexpressed MYC and FOXO1 and downregulated FGFR2 primarily suppress FOXA2, resulting in a loss of its inhibitory function on SNAI1. FOXA2, a transcriptional regulator involving lung and embryonic development, responds to IL-6 induced regulation of fibrinogen synthesis and lung tumor suppression.[106] Downregulated CDK5 and overexpressed NR4A3 and SCARB1 appeared to regulate the overexpressed FOXO1. CDK5 plays roles in cytoskeleton control, cell migration and apoptosis, whereas NR4A3 plays several roles in cancer signaling including transcriptional dysregulation and cell survival.[102]

The overexpression of SNAI1 appeared to associate with signaling that would modulate cancer signaling in MWCNT-exposed cells and was associated with upstream EMT and DNA damage response signaling. Overexpressed ROR1 and under-expressed FOXA2 and DIXDC1, a Wnt pathway modulator, contributed to SNAI1 overexpression. ROR1 participates in Wnt and NFκB signaling pathways, contributes to EMT, and promotes several cancers.[107] Downregulation of ATM, COL1A1 and PLAU, associated with stress response and extracellular matrix processes, appeared to promote downregulation of inflammatory cytokines and mediators including CCL2, CXCL8, TNFAIP3, and POU5F1. Along with the under-expressed ATM, evidence of DNA damage response impacting SNAI1 was observed with overexpressed PRKDC and NDRG1, kinases that associate with DSB repair, mitotic spindle checkpoint, and metastasis disruption.[108, 109] Collectively, these signaling pathways imply that long-term CNM exposure elicited significant DNA damage response[14] and alterations in embryonic signaling, potentially via Wnt and β-catenin pathways that promoted MYC and SNAI1 proto-oncogene signaling that is observed in exposed *in vitro* and *in vivo* models.[110–112]

In summary, we provided evidence that long-term low-dose exposure to CNMs and ASB caused substantial DNA damage and p53 dysregulation in human SAECs. The exposed lung cells exhibited neoplastic and CSC-like properties, as indicated by anchorage-independent colony formation, spheroid formation, anoikis resistance, and CSC markers expression. High

aspect ratio materials including SWCNT, MWCNT and ASB exhibited strong neoplastic and CSC-like properties as compared to low aspect ratio UFCB particles. This result is in good agreement with previous toxicity studies showing enhanced cytotoxicity of high aspect ratio nanomaterials such as nanowires and nanotubes *vs.* low aspect ratio nanomaterials such as round and ringed particles.[113] Likewise, animal studies showed a strong pulmonary inflammatory response to high aspect ratio MWCNT as compared to low aspect ratio MWCNT, which induced no inflammatory response.[114] The impact of aspect ratio on toxicity was also observed in other types of nanoparticles. For example, rod-type aluminum oxide nanoparticles were found to induce a stronger immune response than their spherical counterpart.[115] Despite a vast difference in chemical composition, both ABS (silica-based) and CNTs (carbon-based) induced a similar neoplastic and CSC-like transformation, whereas the low aspect ratio UFCB induced weak effect. Since both UFCB and CNTs used in this study contain >99% carbon and both have minimal metal impurities (i.e. <1%), these results suggest that aspect ratio of nanomaterials is a key determinant of their pathogenicity. Metal impurity and rigidity of nanoparticles may also play a role since ASB, which has a high metal impurity content (38%) and is highly rigid, induced a stronger effect on CSC-like transformation than MWCNT despite having a lower aspect ratio as shown in Table 1. Indeed, previous studies have suggested rigidity as a key factor underlying frustrated phagocytosis caused by rigid fiber-like particles, leading to an elevated and sustained release of pro-inflammatory cytokines and reactive oxygen species that contribute to disease pathogenesis.[116, 117] Our study also unveiled potential molecular mechanisms of CNM-induced neoplastic and CSC-like transformation. It identified self-renewal and EMT-related transcription factors, notably SOX2 and SNAI1 that may serve as key drivers of oncogenic transformation induced by the CNMs.

Acknowledgements

REFERENCES

1. De Volder MF, Tawfick SH, Baughman RH and Hart AJ, Carbon nanotubes: present and future commercial applications, science, 2013, 339, 535–539. [PubMed: 23372006]

2. Schnorr JM and Swager TM, Emerging applications of carbon nanotubes, Chemistry of Materials, 2010, 23, 646–657.

3. Iyiegbuniwe EA, Nwosu UU and Kodali S, A Review of Occupational Health Implications of Exposure and Risk Management of Carbon Nanotubes and Carbon Nanofibers, International Journal of Environmental Science and Development, 2016, 7, 849.

4. Nakanishi J, Morimoto Y, Ogura I, Kobayashi N, Naya M, Ema M, Endoh S, Shimada M, Ogami A and Myojyo T, Risk assessment of the carbon nanotube group, Risk Analysis, 2015, 35, 1940–1956. [PubMed: 25943334]

5. Shvedova AA, Kisin ER, Mercer R, Murray AR, Johnson VJ, Potapovich AI, Tyurina YY, Gorelik O, Arepalli S and Schwegler-Berry D, Unusual inflammatory and fibrogenic pulmonary responses to single-walled carbon nanotubes in mice, American Journal of Physiology-Lung Cellular and Molecular Physiology, 2005, 289, L698–L708. [PubMed: 15951334]

6. Mercer RR, Scabilloni J, Wang L, Kisin E, Murray AR, Schwegler-Berry D, Shvedova AA and Castranova V, Alteration of deposition pattern and pulmonary response as a result of improved dispersion of aspirated single-walled carbon nanotubes in a mouse model, American Journal of Physiology-Lung Cellular and Molecular Physiology, 2008, 294, L87–L97. [PubMed: 18024722]

7. Mercer RR, Hubbs AF, Scabilloni JF, Wang L, Battelli LA, Schwegler-Berry D, Castranova V and Porter DW, Distribution and persistence of pleural penetrations by multi-walled carbon nanotubes, Particle and fibre toxicology, 2010, 7, 28. [PubMed 20920331]

8. Bernstein JMRSM, Bjarne Kjaer Ersboell, Joachim Kunert, David, Biopersistence of synthetic mineral fibers as a predictor of chronic inhalation toxicity in rats, Inhalation toxicology, 2001, 13, 823–849. [PubMed: 11696863]

9. Hesterberg T, Chase G, Axten C, Miller W, Musselman R, Kamstrup O, Hadley J, Morscheidt C, Bernstein D and Thevenaz P, Biopersistence of synthetic vitreous fibers and amosite asbestos in the rat lung following inhalation, Toxicology and applied pharmacology, 1998, 151, 262–275. [PubMed: 9707503]

10. Sargent LM, Porter DW, Staska LM, Hubbs AF, Lowry DT, Battelli L, Siegrist KJ, Kashon ML, Mercer RR and Bauer AK, Promotion of lung adenocarcinoma following inhalation exposure to multi-walled carbon nanotubes, Particle and fibre toxicology, 2014, 11, 3. [PubMed: 24405760]

11. Suzui M, Futakuchi M, Fukamachi K, Numano T, Abdelgied M, Takahashi S, Ohnishi M, Omori T, Tsuruoka S and Hirose A, Multiwalled carbon nanotubes intratracheally instilled into the rat lung induce development of pleural malignant mesothelioma and lung tumors, Cancer science, 2016, 107, 924–935. [PubMed: 27098557]

12. Donaldson K, Poland CA, Murphy FA, MacFarlane M, Chernova T and Schinwald A, Pulmonary toxicity of carbon nanotubes and asbestos—similarities and differences, Advanced drug delivery reviews, 2013, 65, 2078–2086. [PubMed: 23899865]

13. Sargent LM, Shvedova A, Hubbs A, Salisbury J, Benkovic S, Kashon M, Lowry D, Murray A, Kisin E and Friend S, Induction of aneuploidy by single-walled carbon nanotubes, Environmental and molecular mutagenesis, 2009, 50, 708–717. [PubMed: 19774611]

14. Siegrist KJ, Reynolds SH, Kashon ML, Lowry DT, Dong C, Hubbs AF, Young S-H, Salisbury JL, Porter DW and Benkovic SA, Genotoxicity of multi-walled carbon nanotubes at occupationally relevant doses, Particle and fibre toxicology, 2014, 11, 6. [PubMed: 24479647]

15. Jackson P, Hougaard KS, Boisen AMZ, Jacobsen NR, Jensen KA, Møller P, Brunborg G, Gutzkow KB, Andersen O and Loft S, Pulmonary exposure to carbon black by inhalation or instillation in pregnant mice: effects on liver DNA strand breaks in dams and offspring, Nanotoxicology, 2012, 6, 486–500. [PubMed: 21649560]

16. Bernstein C, Prasad AR, Nfonsam V and Bernstein H, in New Research Directions in DNA Repair, InTech, 2013.

17. Shvedova AA, Kisin E, Murray AR, Johnson VJ, Gorelik O, Arepalli S, Hubbs AF, Mercer RR, Keohavong P and Sussman N, Inhalation vs. aspiration of single-walled carbon nanotubes in C57BL/6 mice: inflammation, fibrosis, oxidative stress, and mutagenesis, American Journal of Physiology-Lung Cellular and Molecular Physiology, 2008, 295, L552–L565. [PubMed: 18658273]

18. Shvedova AA, Yanamala N, Kisin ER, Tkach AV, Murray AR, Hubbs A, Chirila MM, Keohavong P, Sycheva LP and Kagan VE, Long-term effects of carbon containing engineered nanomaterials and asbestos in the lung: one year postexposure comparisons, American Journal of Physiology-Lung Cellular and Molecular Physiology, 2013, 306, L170–L182. [PubMed: 24213921]

19. Takagi A, Hirose A, Futakuchi M, Tsuda H and Kanno J, Dose-dependent mesothelioma induction by intraperitoneal administration of multi-wall carbon nanotubes in p53 heterozygous mice, Cancer science, 2012, 103, 1440–1444. [PubMed: 22537085]

20. Snyder-Talkington BN, Pacurari M, Dong C, Leonard SS, Schwegler-Berry D, Castranova V, Qian Y and Guo NL, Systematic analysis of multiwalled carbon nanotube-induced cellular signaling and gene expression in human small airway epithelial cells, toxicological sciences, 2013, 133, 79–89. [PubMed: 23377615]

21. Snyder-Talkington BN, Schwegler-Berry D, Castranova V, Qian Y and Guo NL, Multi-walled carbon nanotubes induce human microvascular endothelial cellular effects in an alveolar-capillary

co-culture with small airway epithelial cells, Particle and fibre toxicology, 2013, 10, 35. [PubMed: 23903001]

22. Borm PJ, Schins RP and Albrecht C, Inhaled particles and lung cancer, part B: paradigms and risk assessment, International Journal of Cancer, 2004, 110, 3–14. [PubMed: 15054863]

23. Pott F, Carcinogenicity study with nineteen granular dusts in rats, Eur J Oncol, 2005, 10, 249–281.

24. Heinrich U, Fuhst R, Rittinghausen S, Creutzenberg O, Bellmann B, Koch W and Levsen K, Chronic inhalation exposure of Wistar rats and two different strains of mice to diesel engine exhaust, carbon black, and titanium dioxide, Inhalation Toxicology, 1995, 7, 533–556.

25. Boffetta P, Soutar A, Cherrie JW, Granath F, Andersen A, Anttila A, Blettner M, Gaborieau V, Klug SJ and Langard S, Mortality among workers employed in the titanium dioxide production industry in Europe, Cancer Causes & Control, 2004, 15, 697–706. [PubMed: 15280628]

26. Ramanakumar AV, Parent MÉ, Latreille B and Siemiatycki J, Risk of lung cancer following exposure to carbon black, titanium dioxide and talc: results from two case–control studies in Montreal, International journal of cancer, 2008, 122, 183–189. [PubMed: 17722096]

27. Le HQ, Tomenson JA, Warheit DB, Fryzek JP, Golden AP and Ellis ED, A Review and Meta-Analysis of Occupational Titanium Dioxide Exposure and Lung Cancer Mortality, Journal of occupational and environmental medicine, 2018, 60, e356–e367. [PubMed: 29538276]

28. Kumar A, Najafzadeh M, Jacob BK, Dhawan A and Anderson D, Zinc oxide nanoparticles affect the expression of p53, Ras p21 and JNKs: an ex vivo/in vitro exposure study in respiratory disease patients, Mutagenesis, 2014, 30, 237–245. [PubMed: 25381309]

29. Wang L, Luanpitpong S, Castranova V, Tse W, Lu Y, Pongrakhananon V and Rojanasakul Y, Carbon nanotubes induce malignant transformation and tumorigenesis of human lung epithelial cells, Nano letters, 2011, 11, 2796–2803. [PubMed: 21657258]

30. Wang L, Stueckle TA, Mishra A, Derk R, Meighan T, Castranova V and Rojanasakul Y, Neoplastic-like transformation effect of single-walled and multi-walled carbon nanotubes compared to asbestos on human lung small airway epithelial cells, Nanotoxicology, 2014, 8, 485–507. [PubMed: 23634900]

31. Dalerba P, Cho RW and Clarke MF, Cancer stem cells: models and concepts, Annu. Rev. Med, 2007, 58, 267–284. [PubMed: 17002552]

32. Wellner U, Schubert J, Burk UC, Schmalhofer O, Zhu F, Sonntag A, Waldvogel B, Vannier C, Darling D and Zur Hausen A, The EMT-activator ZEB1 promotes tumorigenicity by repressing stemness-inhibiting microRNAs, Nature cell biology, 2009, 11, 1487. [PubMed: 19935649]

33. Hadjimichael C, Chanoumidou K, Papadopoulou N, Arampatzi P, Papamatheakis J and Kretsovali A, Common stemness regulators of embryonic and cancer stem cells, World journal of stem cells, 2015, 7, 1150. [PubMed: 26516408]

34. Zhou W, Lv R, Qi W, Wu D, Xu Y, Liu W, Mou Y and Wang L, Snail contributes to the maintenance of stem cell-like phenotype cells in human pancreatic cancer, PloS one, 2014, 9, e87409. [PubMed: 24489910]

35. Luanpitpong S, Li J, Manke A, Brundage K, Ellis E, McLaughlin SL, Angsutararux P, Chanthra N, Voronkova M and Chen YC, SLUG is required for SOX9 stabilization and functions to promote cancer stem cells and metastasis in human lung carcinoma, Oncogene, 2016, 35, 2824. [PubMed: 26387547]

36. Sławek S, Szmyt K, Fularz M, Dziudzia J, Boruczkowski M, Sikora J and Kaczmarek M, Pluripotency transcription factors in lung cancer—a review, Tumor Biology, 2016, 37, 4241–4249. [PubMed: 26581906]

37. Nagata T, Shimada Y, Sekine S, Hori R, Matsui K, Okumura T, Sawada S, Fukuoka J and Tsukada K, Prognostic significance of NANOG and KLF4 for breast cancer, Breast cancer, 2014, 21, 96–101. [PubMed: 22528804]

38. de Resende MF, Chinen LTD, Vieira S, Jampietro J, da Fonseca FP, Vassallo J, Campos LC, Guimarães GC, Soares FA and Rocha RM, Prognostication of OCT4 isoform expression in prostate cancer, Tumor Biology, 2013, 34, 2665–2673. [PubMed: 23636800]

39. Boumahdi S, Driessens G, Lapouge G, Rorive S, Nassar D, Le Mercier M, Delatte B, Caauwe A, Lenglez S and Nkusi E, SOX2 controls tumour initiation and cancer stem-cell functions in squamous-cell carcinoma, Nature, 2014, 511, 246. [PubMed: 24909994]

40. Liu Z, Zhang J, Kang H, Sun G, Wang B, Wang Y and Yang M, Significance of stem cell marker Nanog gene in the diagnosis and prognosis of lung cancer, Oncology letters, 2016, 12, 2507–2510. [PubMed: 27698819]

41. Zhang X, Han B, Huang J, Zheng B, Geng Q, Aziz F and Dong Q, Prognostic significance of OCT4 expression in adenocarcinoma of the lung, Japanese journal of clinical oncology, 2010, 40, 961–966. [PubMed: 20462980]

42. Sholl LM, Long KB and Hornick JL, Sox2 expression in pulmonary non-small cell and neuroendocrine carcinomas, Applied Immunohistochemistry & Molecular Morphology, 2010, 18, 55–61. [PubMed: 19661786]

43. Rudin CM, Durinck S, Stawiski EW, Poirier JT, Modrusan Z, Shames DS, Bergbower EA, Guan Y, Shin J and Guillory J, Comprehensive genomic analysis identifies SOX2 as a frequently amplified gene in small-cell lung cancer, Nature genetics, 2012, 44, 1111. [PubMed: 22941189]

44. Chen S, Xu Y, Chen Y, Li X, Mou W, Wang L, Liu Y, Reisfeld RA, Xiang R and Lv D, SOX2 gene regulates the transcriptional network of oncogenes and affects tumorigenesis of human lung cancer cells, PloS one, 2012, 7, e36326. [PubMed: 22615765]

45. Larsen JE, Nathan V, Osborne JK, Farrow RK, Deb D, Sullivan JP, Dospoy PD, Augustyn A, Hight SK and Sato M, ZEB1 drives epithelial-to-mesenchymal transition in lung cancer, The Journal of clinical investigation, 2016, 126, 3219–3235. [PubMed: 27500490]

46. Yang X, Han M, Han H, Wang B, Li S, Zhang Z and Zhao W, Silencing Snail suppresses tumor cell proliferation and invasion by reversing epithelial-to-mesenchymal transition and arresting G2/M phase in non-small cell lung cancer, International journal of oncology, 2017, 50, 1251–1260. [PubMed: 28259904]

47. Wang L, Castranova V, Mishra A, Chen B, Mercer RR, Schwegler-Berry D and Rojanasakul Y, Dispersion of single-walled carbon nanotubes by a natural lung surfactant for pulmonary in vitro and in vivo toxicity studies, Particle and Fibre Toxicology, 2010, 7, 31. [PubMed: 20958985]

48. Piao CQ, Liu L, Zhao YL, Balajee AS, Suzuki M and Hei TK, Immortalization of human small airway epithelial cells by ectopic expression of telomerase, Carcinogenesis, 2005, 26, 725–731. [PubMed: 15677631]

49. Levina V, Marrangoni AM, DeMarco R, Gorelik E and Lokshin AE, Drug-selected human lung cancer stem cells: cytokine network, tumorigenic and metastatic properties, PloS one, 2008, 3, e3077. [PubMed: 18728788]

50. Pacurari M, Yin XJ, Ding M, Leonard SS, Schwegler-Berry D, Ducatman BS, Chirila M, Endo M, Castranova V and Vallyathan V, Oxidative and molecular interactions of multi-wall carbon nanotubes (MWCNT) in normal and malignant human mesothelial cells, Nanotoxicology, 2008, 2, 155–170.

51. Porter DW, Hubbs AF, Mercer RR, Wu N, Wolfarth MG, Sriram K, Leonard S, Battelli L, Schwegler-Berry D and Friend S, Mouse pulmonary dose-and time course-responses induced by exposure to multi-walled carbon nanotubes, Toxicology, 2010, 269, 136–147. [PubMed: 19857541]

52. Mishra A, Rojanasakul Y, Chen BT, Castranova V, Mercer RR and Wang L, Assessment of pulmonary fibrogenic potential of multiwalled carbon nanotubes in human lung cells, Journal of Nanomaterials, 2012, 2012, 4.

53. Msiska Z, Pacurari M, Mishra A, Leonard SS, Castranova V and Vallyathan V, DNA double-strand breaks by asbestos, silica, and titanium dioxide: possible biomarker of carcinogenic potential?, American journal of respiratory cell and molecular biology, 2010, 43, 210–219. [PubMed: 19783790]

54. Stone KC, Mercer RR, Gehr P, Stockstill B and Crapo JD, Allometric relationships of cell numbers and size in the mammalian lung, Am J Respir Cell Mol Biol, 1992, 6, 235–243. [PubMed: 1540387]

55. Colburn NH, Bruegge WV, Bates J, Gray R, Rossen J, Kelsey W and Shimada T, Correlation of anchorage-independent growth with tumorigenicity of chemically transformed mouse epidermal cells, Cancer research, 1978, 38, 624–634. [PubMed: 626967]

56. Horibata S, Vo TV, Subramanian V, Thompson PR and Coonrod SA, Utilization of the soft agar colony formation assay to identify inhibitors of tumorigenicity in breast cancer cells, JoVE (Journal of Visualized Experiments), 2015, e52727. [PubMed: 26067809]

57. Burmeister B, Schwerdtle T, Poser I, Hoffmann E, Hartwig A, Müller W-U, Rettenmeier A, Seemayer N and Dopp E, Effects of asbestos on initiation of DNA damage, induction of DNA-strand breaks, P53-expression and apoptosis in primary, SV40-transformed and malignant human mesothelial cells, Mutation Research/Genetic Toxicology and Environmental Mutagenesis, 2004, 558, 81–92.

58. Kuo LJ and Yang L-X, γ-H2AX-a novel biomarker for DNA double-strand breaks, In vivo, 2008, 22, 305–309. [PubMed: 18610740]

59. Tu W-Z, Li B, Huang B, Wang Y, Liu X-D, Guan H, Zhang S-M, Tang Y, Rang W-Q and Zhou P-K, γH2AX foci formation in the absence of DNA damage: Mitotic H2AX phosphorylation is mediated by the DNA-PKcs/CHK2 pathway, FEBS letters, 2013, 587, 3437–3443. [PubMed: 24021642]

60. Williams AB and Schumacher B, p53 in the DNA-damage-repair process, Cold Spring Harbor perspectives in medicine, 2016, a026070. [PubMed: 27048304]

61. Olivier M, Hollstein M and Hainaut P, TP53 mutations in human cancers: origins, consequences, and clinical use, Cold Spring Harbor perspectives in biology, 2009, a001008.

62. Rich JN, Cancer stem cells: understanding tumor hierarchy and heterogeneity, Medicine, 2016, 95.

63. Pongrakhananon V, Luanpitpong S, Stueckle TA, Wang L, Nimmannit U and Rojanasakul Y, Carbon nanotubes induce apoptosis resistance of human lung epithelial cells through FLICE-inhibitory protein, Toxicological Sciences, 2014, 143, 499–511. [PubMed: 25412619]

64. Luanpitpong S, Wang L, Castranova V and Rojanasakul Y, Induction of stem-like cells with malignant properties by chronic exposure of human lung epithelial cells to single-walled carbon nanotubes, Particle and fibre toxicology, 2014, 11, 22. [PubMed: 24885671]

65. Qiu Z-X, Zhao S, Mo X-M and Li W-M, Overexpression of PROM1 (CD133) confers poor prognosis in non-small cell lung cancer, International journal of clinical and experimental pathology, 2015, 8, 6589. [PubMed: 26261540]

66. Cortes-Dericks L, Galetta D, Spaggiari L, Schmid RA and Karoubi G, High expression of octamer-binding transcription factor 4A, prominin-1 and aldehyde dehydrogenase strongly indicates involvement in the initiation of lung adenocarcinoma resulting in shorter disease-free intervals, European journal of cardio-thoracic surgery, 2012, 41, e173–e181. [PubMed: 22529186]

67. Eramo A, Lotti F, Sette G, Pilozzi E, Biffoni M, Di Virgilio A, Conticello C, Ruco L, Peschle C and De Maria R, Identification and expansion of the tumorigenic lung cancer stem cell population, Cell death and differentiation, 2008, 15, 504. [PubMed: 18049477]

68. Mohyeldin A, Garzón-Muvdi T and Quiñones-Hinojosa A, Oxygen in stem cell biology: a critical component of the stem cell niche, Cell stem cell, 2010, 7, 150–161. [PubMed: 20682444]

69. Hardavella G, George R and Sethi T, Lung cancer stem cells—characteristics, phenotype, Translational lung cancer research, 2016, 5, 272. [PubMed: 27413709]

70. Prabavathy D, Swarnalatha Y and Ramadoss N, Lung cancer stem cells—origin, characteristics and therapy, Stem cell investigation, 2018, 5.

71. Li G, Gao Y, Cui Y, Zhang T, Cui R, Jiang Y and Shi J, Overexpression of CD44 is associated with the occurrence and migration of non-small cell lung cancer, Molecular medicine reports, 2016, 14, 3159–3167. [PubMed: 27573351]

72. Li F, Zeng H and Ying K, The combination of stem cell markers CD133 and ABCG2 predicts relapse in stage I non-small cell lung carcinomas, Medical oncology, 2011, 28, 1458–1462. [PubMed: 20717756]

73. Liu X and Fan D, The epithelial-mesenchymal transition and cancer stem cells: functional and mechanistic links, Current pharmaceutical design, 2015, 21, 1279–1291. [PubMed: 25506898]

74. Que J, Luo X, Schwartz RJ and Hogan BL, Multiple roles for Sox2 in the developing and adult mouse trachea, Development, 2009, 136, 1899–1907. [PubMed: 19403656]

75. Tompkins DH, Besnard V, Lange AW, Wert SE, Keiser AR, Smith AN, Lang R and Whitsett JA, Sox2 is required for maintenance and differentiation of bronchiolar Clara, ciliated, and goblet cells, PloS one, 2009, 4, e8248. [PubMed: 20011520]

76. Chou YT, Lee CC, Hsiao SH, Lin SE, Lin SC, Chung CH, Chung CH, Kao YR, Wang YH and Chen CT, The emerging role of SOX2 in cell proliferation and survival and its crosstalk with oncogenic signaling in lung cancer, Stem cells, 2013, 31, 2607–2619. [PubMed: 23940081]

77. Correia LL, Johnson J-A, McErlean P, Bauer J, Farah H, Rassl DM, Rintoul RC, Sethi T, Lavender P and Rawlins EL, SOX2 drives bronchial dysplasia in a novel organotypic model of early human squamous lung cancer, American journal of respiratory and critical care medicine, 2017, 195, 1494–1508. [PubMed: 28199128]

78. Mani SA, Guo W, Liao M-J, Eaton EN, Ayyanan A, Zhou AY, Brooks M, Reinhard F, Zhang CC and Shipitsin M, The epithelial-mesenchymal transition generates cells with properties of stem cells, Cell, 2008, 133, 704–715. [PubMed: 18485877]

79. Sun Y, Song GD, Sun N, Chen JQ and Yang SS, Slug overexpression induces stemness and promotes hepatocellular carcinoma cell invasion and metastasis, Oncology letters, 2014, 7, 1936–1940. [PubMed: 24932263]

80. Zhou C, Jiang H, Zhang Z, Zhang G, Wang H, Zhang Q, Sun P, Xiang R and Yang S, ZEB1 confers stem cell-like properties in breast cancer by targeting neurogenin-3, Oncotarget, 2017, 8, 54388. [PubMed: 28903350]

81. Yilmaz M and Christofori G, Mechanisms of motility in metastasizing cells, Molecular cancer research, 2010, 1541–7786. MCR-1510–0139.

82. Yanagawa J, Walser TC, Zhu LX, Hong L, Fishbein MC, Mah V, Chia D, Goodglick L, Elashoff DA and Luo J, Snail promotes CXCR2 ligand–dependent tumor progression in non–small cell lung carcinoma, Clinical Cancer Research, 2009, 1078–0432. CCR-1009–1558.

83. Zhang J, Lu C, Zhang J, Kang J, Cao C and Li M, Involvement of ZEB1 and E-cadherin in the invasion of lung squamous cell carcinoma, Molecular biology reports, 2013, 40, 949–956. [PubMed: 23065281]

84. Merikallio H, Slug is associated with poor survival in squamous cell carcinoma of the lung, International journal of clinical and experimental pathology, 2014, 7, 5846. [PubMed: 25337226]

85. Takeyama Y, Sato M, Horio M, Hase T, Yoshida K, Yokoyama T, Nakashima H, Hashimoto N, Sekido Y and Gazdar AF, Knockdown of ZEB1, a master epithelial-to-mesenchymal transition (EMT) gene, suppresses anchorage-independent cell growth of lung cancer cells, Cancer letters, 2010, 296, 216–224. [PubMed: 20452118]

86. Clarhaut J, Gemmill RM, Potiron VA, Ait-Si-Ali S, Imbert J, Drabkin HA and Roche J, ZEB-1, a repressor of the semaphorin 3F tumor suppressor gene in lung cancer cells, Neoplasia, 2009, 11, IN2–IN5.

87. Yang L, Amann JM, Kikuchi T, Porta R, Guix M, Gonzalez A, Park K-H, Billheimer D, Arteaga CL and Tai H-H, Inhibition of epidermal growth factor receptor signaling elevates 15-hydroxyprostaglandin dehydrogenase in non–small-cell lung cancer, Cancer research, 2007, 67, 5587–5593. [PubMed: 17575121]

88. Chakraborty S, Pandita RK, Hambarde S, Mattoo AR, Charaka V, Ahmed KM, Iyer SP, Hunt CR and Pandita TK, SMARCAD1 Phosphorylation and Ubiquitination Are Required for Resection during DNA Double-Strand Break Repair, iScience, 2018, 2, 123–135. [PubMed: 29888761]

89. Fontana GA, Reinert JK, Thomä NH and Rass U, Shepherding DNA ends: Rif1 protects telomeres and chromosome breaks, Microbial Cell, 2018, 5, 327. [PubMed: 29992129]

90. Xiao S, Lu J, Sridhar B, Cao X, Yu P, Zhao T, Chen C-C, McDee D, Sloofman L and Wang Y, SMARCAD1 contributes to the regulation of naive Pluripotency by interacting with Histone Citrullination, Cell reports, 2017, 18, 3117–3128. [PubMed: 28355564]

91. Pitroda SP, Pashtan IM, Logan HL, Budke B, Darga TE, Weichselbaum RR and Connell PP, DNA repair pathway gene expression score correlates with repair proficiency and tumor sensitivity to chemotherapy, Science translational medicine, 2014, 6, 229ra242–229ra242.

92. Wei H, Liang F, Cheng W, Zhou R, Wu X, Feng Y and Wang Y, The mechanisms for lung cancer risk of PM2. 5: Induction of epithelial-mesenchymal transition and cancer stem cell properties in human non-small cell lung cancer cells, Environmental toxicology, 2017, 32, 2341–2351. [PubMed: 28846189]

93. Zakaria N, Yusoff NM, Zakaria Z, Lim MN, Baharuddin PJN, Fakiruddin KS and Yahaya B, Human non-small cell lung cancer expresses putative cancer stem cell markers and exhibits the transcriptomic profile of multipotent cells, BMC cancer, 2015, 15, 84. [PubMed: 25881239]

94. Park E, Park SY, Sun P-L, Jin Y, Kim JE, Jheon S, Kim K, Lee CT, Kim H and Chung J-H, Prognostic significance of stem cell-related marker expression and its correlation with histologic subtypes in lung adenocarcinoma, Oncotarget, 2016, 7, 42502. [PubMed: 27285762]

95. Li X, Zhou X, Li Y, Zu L, Pan H, Liu B, Shen W, Fan Y and Zhou Q, Activating transcription factor 3 promotes malignance of lung cancer cells in vitro, Thoracic cancer, 2017, 8, 181–191. [PubMed: 28239957]

96. Zhang Z, Newton K, Kummerfeld SK, Webster J, Kirkpatrick DS, Phu L, Eastham-Anderson J, Liu J, Lee WP and Wu J, Transcription factor Etv5 is essential for the maintenance of alveolar type II cells, Proceedings of the National Academy of Sciences, 2017, 201621177.

97. Balasooriya G, Goschorska M, Piddini E and Rawlins EL, FGFR2 is required for airway basal cell self-renewal and terminal differentiation, Development, 2017, dev. 135681.

98. Boufraqech M, Wei D, Weyemi U, Zhang L, Quezado M, Kalab P and Kebebew E, LOX is a novel mitotic spindle-associated protein essential for mitosis, Oncotarget, 2016, 7, 29023. [PubMed: 27296552]

99. Sato T and Sekido Y, NF2/Merlin Inactivation and Potential Therapeutic Targets in Mesothelioma, International journal of molecular sciences, 2018, 19, 988.

100. Poh AR, O'Donoghue RJ and Ernst M, Hematopoietic cell kinase (HCK) as a therapeutic target in immune and cancer cells, Oncotarget, 2015, 6, 15752. [PubMed: 26087188]

101. Shy BR, Wu C-I, Khramtsova GF, Zhang JY, Olopade OI, Goss KH and Merrill BJ, Regulation of Tcf7l1 DNA binding and protein stability as principal mechanisms of Wnt/β-catenin signaling, Cell reports, 2013, 4, 1–9. [PubMed: 23810553]

102. Beard JA, Tenga A and Chen T, The interplay of NR4A receptors and the oncogene–tumor suppressor networks in cancer, Cellular signalling, 2015, 27, 257–266. [PubMed: 25446259]

103. Yoshida GJ, Emerging roles of Myc in stem cell biology and novel tumor therapies, Journal of Experimental & Clinical Cancer Research, 2018, 37, 173. [PubMed: 30053872]

104. Kumar M, Allison DF, Baranova NN, Wamsley JJ, Katz AJ, Bekiranov S, Jones DR and Mayo MW, NF-κB regulates mesenchymal transition for the induction of non-small cell lung cancer initiating cells, PLoS One, 2013, 8, e68597. [PubMed: 23935876]

105. van Schaijik B, Davis PF, Wickremesekera AC, Tan ST and Itinteang T, Subcellular localisation of the stem cell markers OCT4, SOX2, NANOG, KLF4 and c-MYC in cancer: a review, Journal of clinical pathology, 2018, 71, 88–91. [PubMed: 29180509]

106. Jang S-M, An J-H, Kim C-H, Kim J-W and Choi K-H, Transcription factor FOXA2-centered transcriptional regulation network in non-small cell lung cancer, Biochemical and biophysical research communications, 2015, 463, 961–967. [PubMed: 26093302]

107. Borcherding N, Kusner D, Liu G-H and Zhang W, ROR1, an embryonic protein with an emerging role in cancer biology, Protein & cell, 2014, 5, 496–502. [PubMed: 24752542]

108. Fang BA, Kova evi Ž, Park KC, Kalinowski DS, Jansson PJ, Lane DJ, Sahni S and Richardson DR, Molecular functions of the iron-regulated metastasis suppressor, NDRG1, and its potential as a molecular target for cancer therapy, Biochimica et Biophysica Acta (BBA)-Reviews on Cancer, 2014, 1845, 1–19. [PubMed: 24269900]

109. Zhou Z, Patel M, Ng N, Hsieh MH, Orth AP, Walker JR, Batalov S, Harris JL and Liu J, Identification of synthetic lethality of PRKDC in MYC-dependent human cancers by pooled shRNA screening, BMC cancer, 2014, 14, 944. [PubMed: 25495526]

110. Poulsen SS, Saber AT, Williams A, Andersen O, Købler C, Atluri R, Pozzebon ME, Mucelli SP, Simion M and Rickerby D, MWCNTs of different physicochemical properties cause similar inflammatory responses, but differences in transcriptional and histological markers of fibrosis in mouse lungs, Toxicology and applied pharmacology, 2015, 284, 16–32. [PubMed: 25554681]

111. Polimeni M, Gulino GR, Gazzano E, Kopecka J, Marucco A, Fenoglio I, Cesano F, Campagnolo L, Magrini A and Pietroiusti A, Multi-walled carbon nanotubes directly induce epithelial-mesenchymal transition in human bronchial epithelial cells via the TGF-β-mediated Akt/GSK-3β/SNAIL-1 signalling pathway, Particle and fibre toxicology, 2015, 13, 27.

112. Roudi R, Madjd Z, Ebrahimi M, Najafi A, Korourian A, Shariftabrizi A and Samadikuchaksaraei A, Evidence for embryonic stem-like signature and epithelial-mesenchymal transition features in the spheroid cells derived from lung adenocarcinoma, Tumor Biology, 2016, 37, 11843–11859. [PubMed: 27048287]

113. Buzea C, Pacheco II and Robbie K, Nanomaterials and nanoparticles: sources and toxicity, Biointerphases, 2007, 2, MR17–MR71. [PubMed: 20419892]

114. Poland CA, Duffin R, Kinloch I, Maynard A, Wallace WA, Seaton A, Stone V, Brown S, MacNee Wand Donaldson K, Carbon nanotubes introduced into the abdominal cavity of mice show asbestos-like pathogenicity in a pilot study, Nature nanotechnology, 2008, 3, 423.

115. Park E-J, Kim SN, Kang M-S, Lee B-S, Yoon C, Jeong U, Kim Y, Lee G-H, Kim D-W and Kim JS, A higher aspect ratio enhanced bioaccumulation and altered immune responses due to intravenously-injected aluminum oxide nanoparticles, Journal of immunotoxicology, 2016, 13, 439–448. [PubMed: 27042761]

116. Brown D, Kinloch I, Bangert U, Windle A, Walter D, Walker G, Scotchford C, Donaldson K and Stone V, An in vitro study of the potential of carbon nanotubes and nanofibres to induce inflammatory mediators and frustrated phagocytosis, Carbon, 2007, 45, 1743–1756.

117. Padmore T, Stark C, Turkevich LA and Champion JA, Quantitative analysis of the role of fiber length on phagocytosis and inflammatory response by alveolar macrophages, Biochimica et Biophysica Acta (BBA)-General Subjects, 2017, 1861, 58–67. [PubMed: 27784615]

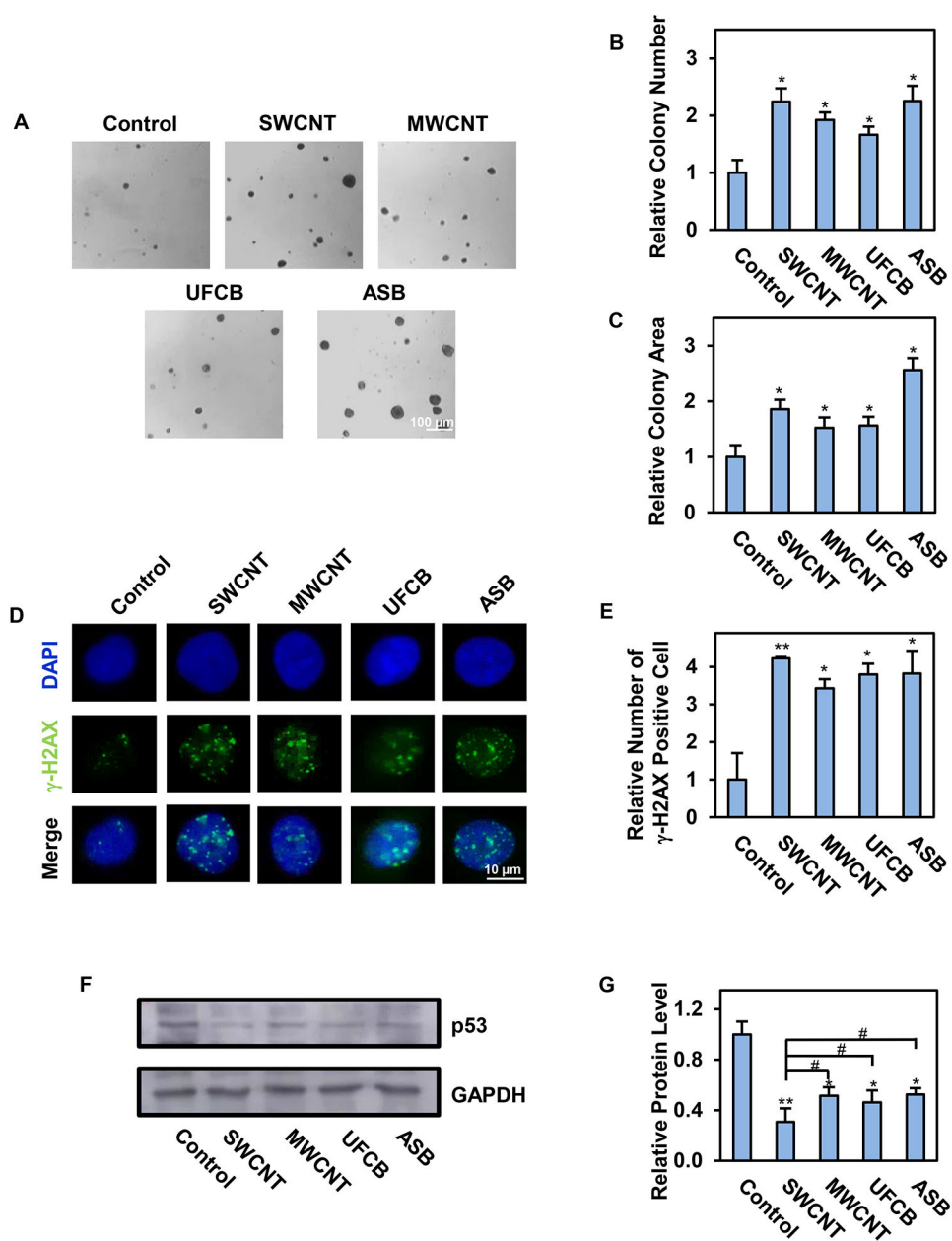Author Manuscript

Author Manuscript

Author Manuscript

Author Manuscript

Fig. 1.

Long-term exposure to single-walled carbon nanotube (SWCNT), multi-walled carbon nanotube (MWCNT), ultrafine carbon black (UFCB) or crocidolite asbestos (ASB) induces irreversible neoplastic-like transformation and DNA double-strand break. Human small airway epithelial cells (SAECs) were continuously exposed to the tested particles for 6 months in culture. They were then examined for neoplastic-like transformation and DNA double strand break by soft-agar colony formation and γ-H2AX assay. A-C: Representative images and quantification of colonies formed by the exposed cells on soft agar after 28 days. Scale bar is 100 μm. 100X magnification.; D-E: Representative immunofluorescence images and quantification of phosphorylated histone H2AX (γ-H2AX) foci in the exposed cells. Scale bar is 10 μm. 200X magnification. Quantification of γ-H2AX positive cells with >5
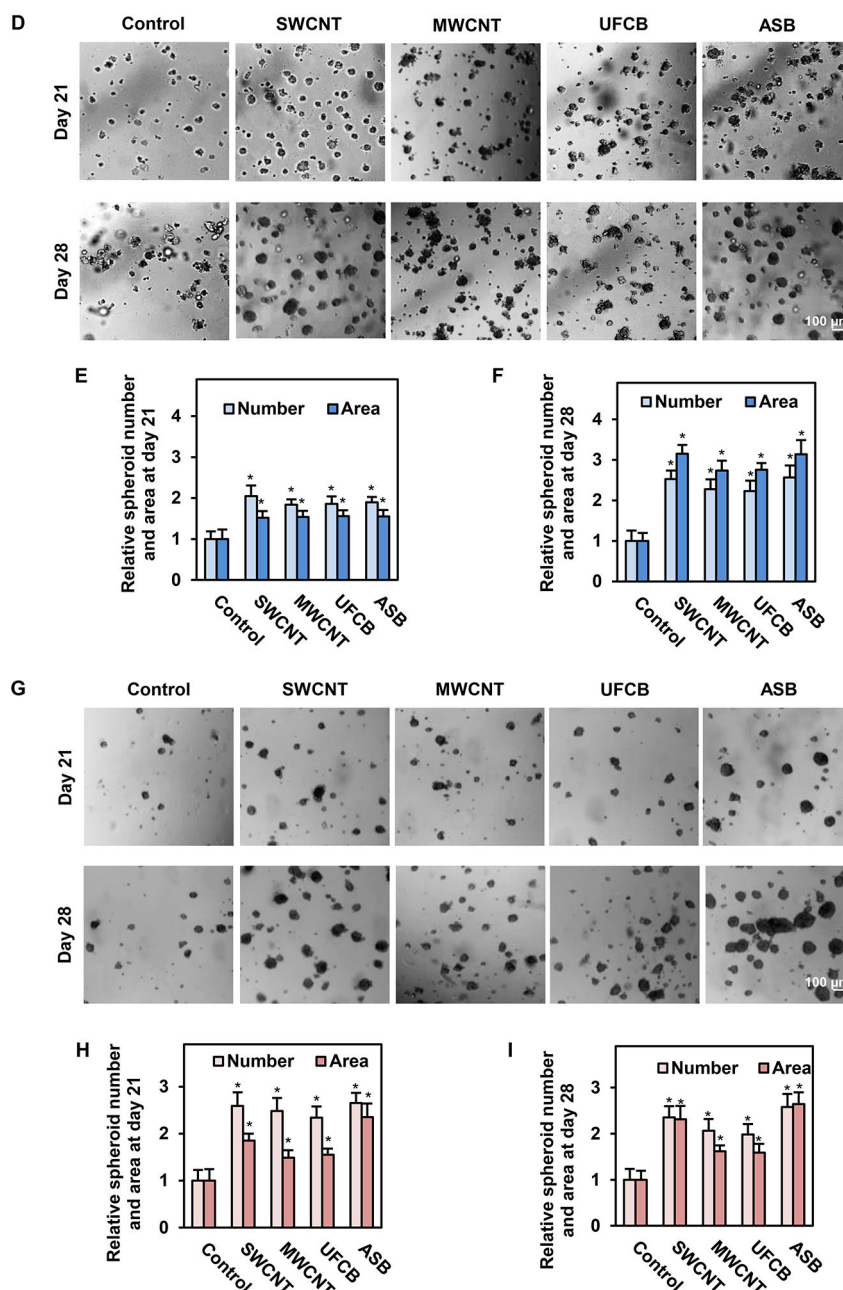
foci/cell is shown; F-G: Representative Western blotting and quantification of p53 protein in the exposed cells. Data are presented as relative values to passage-matched control cells treated with particle-free medium. Data are mean ± SD (n=4), $*p < 0.05$, $**p < 0.01$ versus control cells. [#]$p < 0.05$ versus SWCNT-exposed cells.

Fig. 2.

Long-term exposure to SWCNT, MWCNT, UFCB or ASB induces anoikis resistance and cancer stem cell-like phenotype. Particle-exposed SAECs were grown under non-adherent conditions and analyzed for anoikis or detachment-induced cell death. A: Viability of the exposed cells after detachment as a function of time, determined by MTS assay; B: Percentage of apoptotic cells after detachment determined by Hoechst 33342 assay, and C: Representative images of Hoechst 33342 stained cells. Apoptotic nuclei are brightly fluorescent due to DNA condensation, which is a characteristic of apoptotic cells; D: Representative images of primary 3D spheroids from particle-exposed cells under non-

adherent conditions. Images were captured at 21 and 28 days post-plating; E-F: Quantification of the primary spheroids; G: Images of secondary spheroids captured at 21 and 28 days post-plating; H-I: Quantification of the secondary spheroids. Scale bar is 100 µm. 100X magnification. Data are presented as relative values to passage-matched control cells. Data are mean ± SD (n=4), *$p < 0.05$ versus control cells.
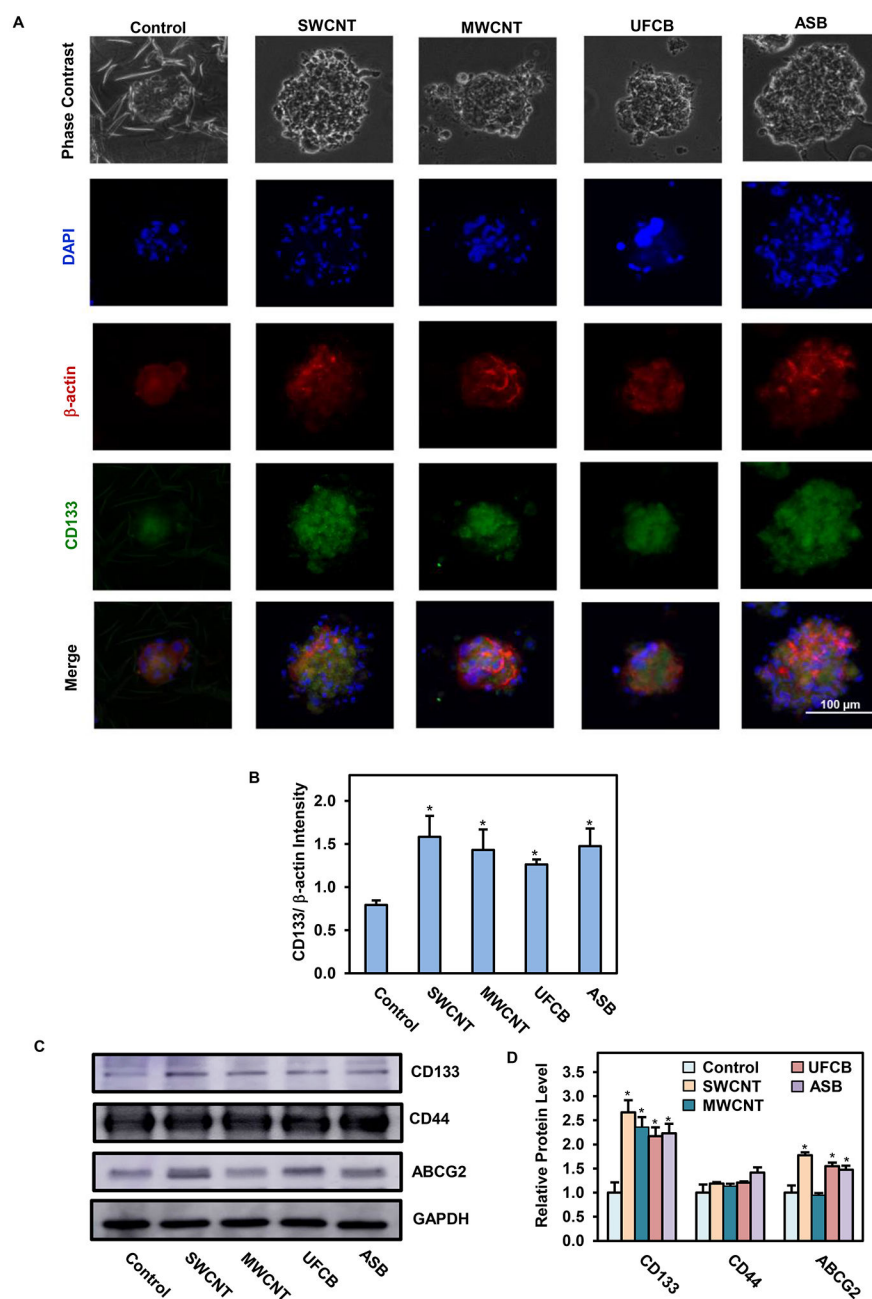
Fig. 3.
Expression of stem cell markers in SWCNT, MWCNT, UFCB, and ASB-exposed cells. A: Representative immunofluorescence images of secondary spheroids at day 28 showing CD133 stem cell marker (green), β-actin (red), and nucleus (DAPI blue) staining. Scale bar is 100 μm. 200X magnification.; B: Quantification of CD133 fluorescence intensity normalized to β-actin intensity using image analysis software; C-D: Western blot analysis and quantification of stem cell markers CD133, CD44 and ABCG2 in particle-exposed cells under normal cell culture conditions. Data are presented as relative values to passage-
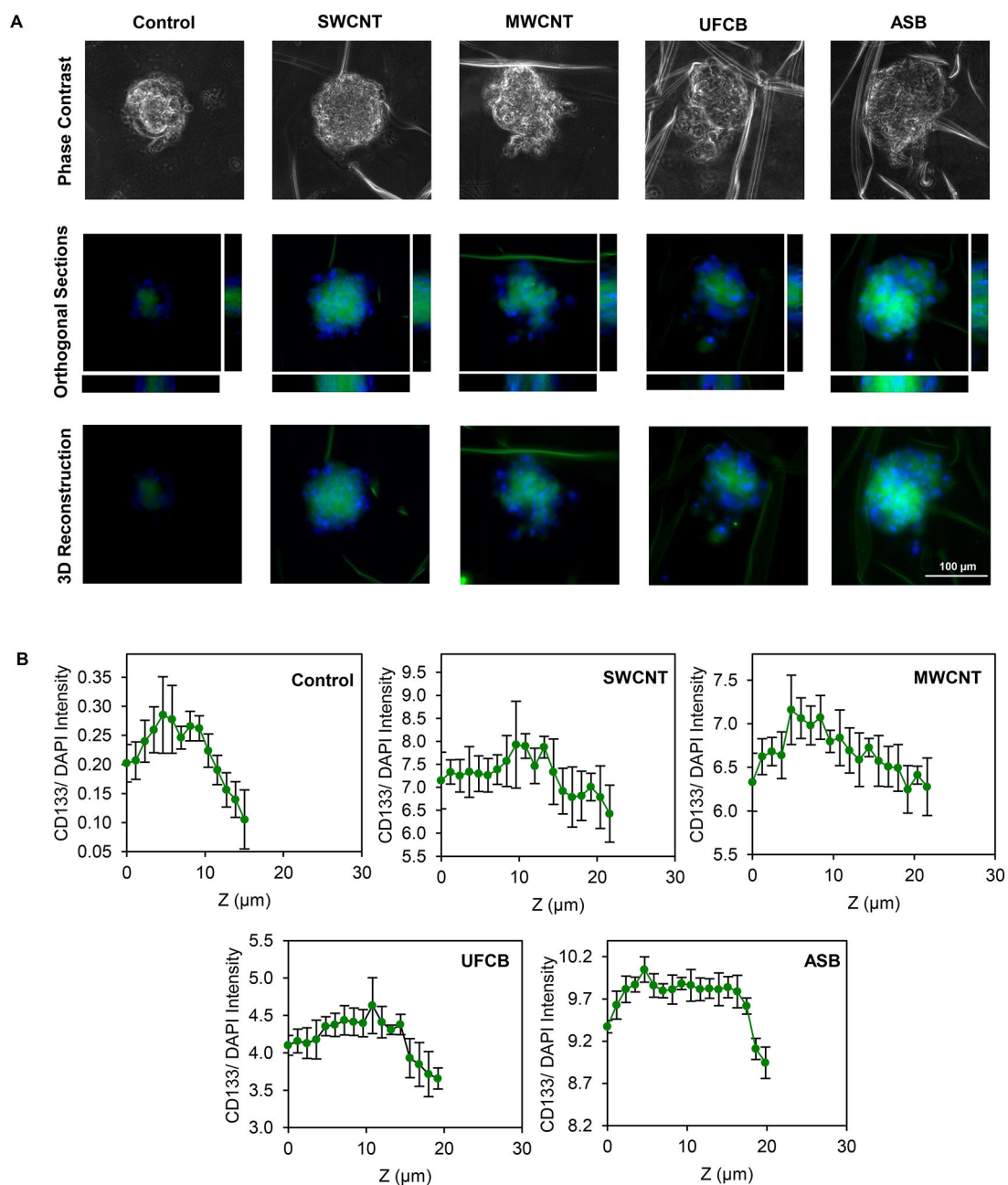
matched control cells. Data are mean ± SD (n=3), *$p < 0.05$ versus passage-matched control cells.

Fig. 4.
Distribution of stem cell marker in spheroids from particle-exposed cells. A: Representative 3D immunofluorescence images and orthogonal sections of secondary spheroids at day 28, stained for CD133 (green) and nucleus (DAPI); B: Quantification of CD133 intensity along z-axis normalized to DAPI intensity using image analysis software. Scale bar is 100 μm. 200X magnification. Data are mean ± SD (n=3).
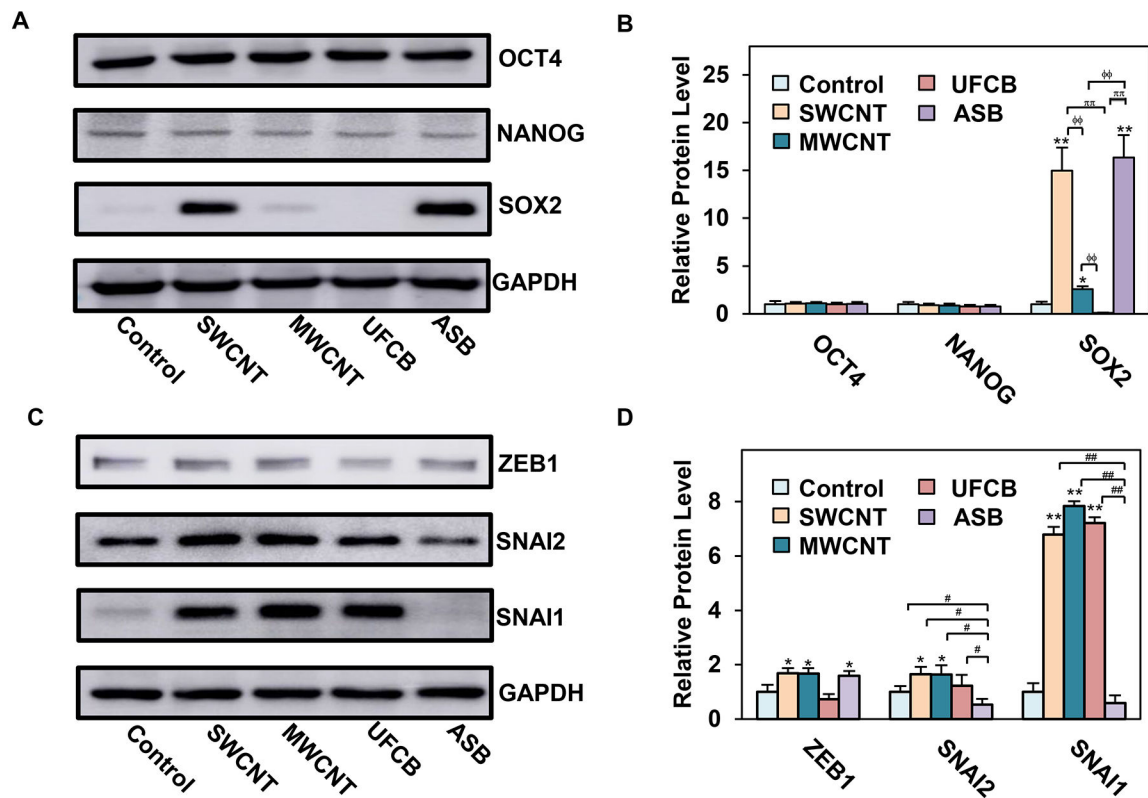
Fig. 5.
Long-term exposure to SWCNT, MWCNT, UFCB or ASB induces self-renewal and EMT-activating transcription factors. A-B: Western blot analysis and quantification of self-renewal transcription factors OCT4, NANOG, and SOX2 in particle-exposed SAECs; C-D: Western blot analysis and quantification of EMT-activating transcription factors ZEB1, SNAI2, and SNAI1. Data are mean ± SD (n=3). $**p < 0.01$, $*p < 0.05$ control cells. $^{\phi\phi}p < 0.01$ versus MWCNT-exposed cells. $^{\pi\pi}p < 0.01$ versus UFCB-exposed cells. $^{\#\#}p < 0.01$, $^{\#}p < 0.05$, versus ASB-exposed cells.
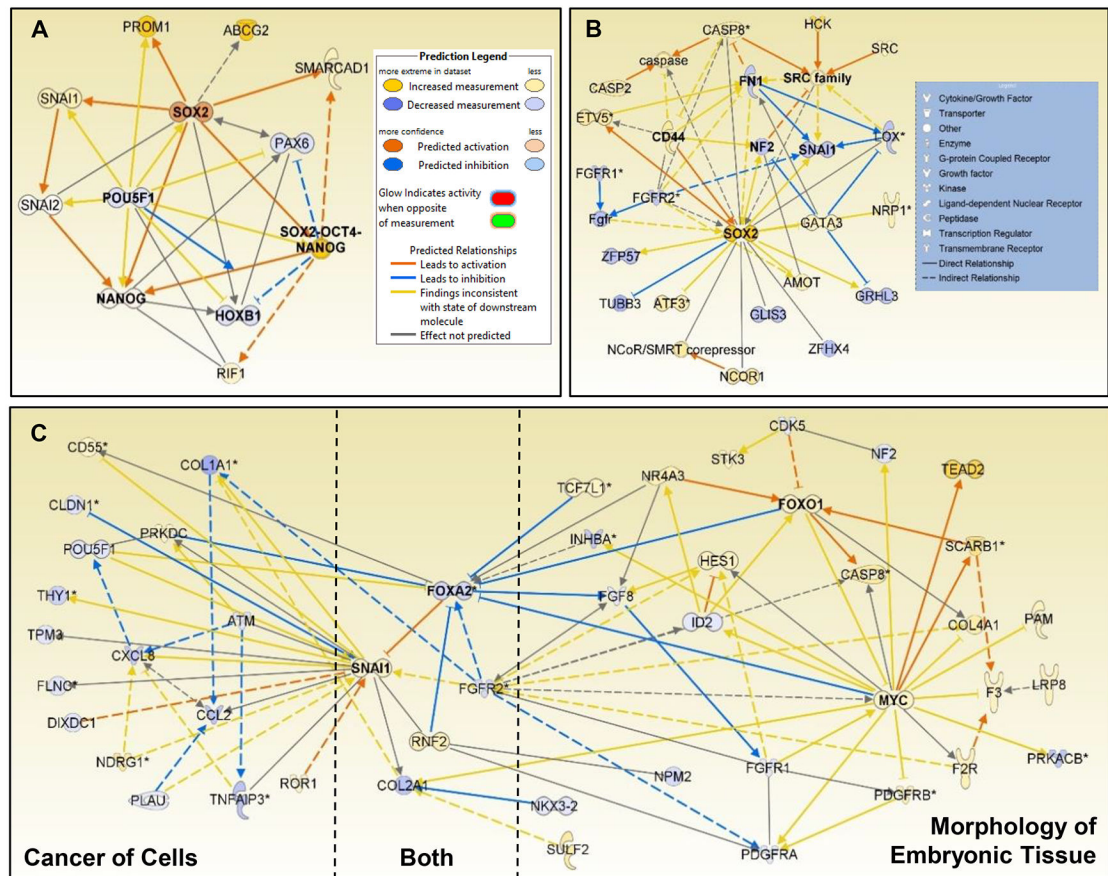
Fig. 6.
Gene signaling networks of SOX2 and SNAI1 signaling associated with stem cell and cancer signaling. A: Activated SOX2 in SWCNT-transformed cells associated with known stem cell signaling; B: SOX2 was involved in crosstalk between development and pro-cancer signaling in ASB-transformed cells; C: SNAI1 and FOXA2 signaling served as crosstalk hubs between MYC-mediated embryonic morphology and cancer signaling in MWCNT-transformed cells.

Table 1.

Physicochemical properties of particles used in this study

Properties	SWCNT	MWCNT	UFCB	ASB
BET surface area (m^2/g) *	400–1040	26	43	9.8
Dry mean width (nm)	1–4	81 ± 5	37	210
Dry mean length (μm)	1–4	8.19 ± 1.7	n/a $^\pi$	10
Dispersed mean width (nm)	270	78	700	210
Dispersed mean length (μm)	1.08	5.1	0.93	10
Aspect ratio	~1,000	−100	~1	47.6
Hydrodynamic mean diameter (nm)	122.5±83.8	163.3± 55.1	126.7±26.7	144.9±59.9
Zeta potential (mV)	−17.1±0.1	−17.6±1	−15.4±1.4	−18.4±1.4
% Carbon (w/w)	99	99	>99	<1
% Metal impurities (w/w)	<1	0.78	<1	50.9 for SiO2, 38 for other metals
Major metal impurities	0.23% Fe	0.41% Na, 0.32% Fe	0.0011% Fe	31.8% Fe, 5.3% Na, 0.8% Mg

* Brunauer-Emmett-Teller nitrogen absorption method.

$^\pi$ Spherical shaped